PERFORMANCE INVESTIGATIONS OF SWITCHED RELUCTANCE MOTOR DRIVE

A DISSERTATION

Submitted in partial fulfillment of the requirements for the award of the degree of

MASTER OF TECHNOLOGY

in

ELECTRICAL ENGINEERING

(With Specialization in Power Apparatus and Electric Drives)

By

ANVESH GOUD MEDI

DEPARTMENT OF ELECTRICAL ENGINEERING
INDIAN INSTITUTE OF TECHNOLOGY ROORKEE
ROORKEE -247 667 (INDIA)
JUNE, 2007

D No.-M.T

CANDIDATE'S DECLARATION

I hereby declare that the work that is being presented in this dissertation report entitled **"PERFORMANCE INVESTIGATIONS ON SWITCHED RELUCTANCE MOTOR DRIVE"** submitted in partial fulfillment of the requirements for the award of the degree of **Master Of Technology** with specialization in **Power Apparatus and Electric Drives,** to the **Department Of Electrical Engineering, Indian Institute Of Technology, Roorkee**, is an authentic record of my own work carried out, under the guidance of **Dr. Pramod Agrawal**, Professor, Department of Electrical Engineering.

The matter embodied in this dissertation report has not been submitted by me for the Award of any other degree or diploma.

Date: 29/6/'07
Place: Roorkee

(ANVESH GOUD MEDI)

This is to certify that the above statement made by the candidate is correct to the best of my knowledge.

(DR. PRAMOD AGRAWAL)
Professor,
Department of Electrical Engineering,
Indian Institute of Technology,
ROORKEE – 247 667,
INDIA.

ACKNOWLEDGEMENT

I wish to express my deep sense of gratitude and sincere thanks to my beloved guide **Dr.** Pramod Agrawal, Prof., Department of Electrical Engineering, IIT Roorkee, for being helpful and a great source of inspiration. I wish to extend my sincere thanks for his excellent guidance and suggestions during the dissertation work.

I am thankful to Mr. Abdul Hamid Bhat and Mr. Kalpesh Bhalodi, Ph.D Research scholars for their valuable guidance and suggestions during the work.

I also express sincere thanks to all staff members of Drives lab and Electric workshop for their help in completion of this work.

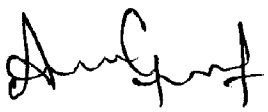

(ANVESH GOUD MEDI)

ABSTRACT

The switched reluctance motor (SRM) drive is receiving increasing attention from various researchers as well as industry as a viable candidate for adjustable speed and servo applications. The switched reluctance motor is simple in construction. It not only features a salient pole stator with concentrated coils, but also features a salient pole rotor, which has no conductors or magnets and is thus the simplest of all electric machine rotors. Combining the unique features of an SRM with simple and efficient power converter that it uses, a superior motor drive system emerges which may be preferable for many applications compared to other ac or dc motor drive systems.

In this thesis, simulation of the current and speed controlled SRM drive is carried for various operating conditions by changing the load and the reference quantities. The performance of the drive is investigated for different switching angles .The optimum turn off angle for a particular load is determined. Different modeling approaches and simulation models of SRM are presented. Implementation of microcontroller controlled SRM drive is done experimentally. The starting problem for an SRM is presented with a solution. Finally, the flowcharts for the open loop operation and current controlled operation of the drive are given.

CONTENTS

The Variable Reluctance Motor is being used in many commercially adjustable speed applications since 1969; due to its unique mechanical structure and simple power electronic drive requirements. The intrinsic simplicity and ruggedness make it superior to other electric machines. Because unidirectional current is required from the converter, only one switch per phase is needed. Even though some converters use more than one switches to increase the reliability or to realize certain control strategies that are not possible by using only one switch per phase. In addition, each phase winding of the SRM is independent; so, it can operate with some of the phase windings disabled, at a lower power output.

It is a doubly salient machine with salient poles on both stator and rotor. The stator has wound field coils as such of a DC machine and the rotor has no coils or magnets. The rotor is aligned whenever diametrically opposite stator poles are exited. In a magnetic circuit, the rotating member prefers to come to the minimum reluctance position at the instance of excitation. While two rotor poles are aligned to the two stator poles, another set of rotor poles is out of alignment with respect to a different set of stator poles. Then, this set of stator poles is exited to bring the rotor poles into alignment. Likewise, by sequentially switching the currents into the stator windings, the rotor is rotated. The movement of the rotor, hence the production of torque and power, involves switching of currents into stator windings when there is a variation of reluctance. This is the reason for considering this variable speed motor drive as a Switched Reluctance Motor drive.

1.1 Importance of SRM

SRM drives are beginning to penetrate the growing market of adjustable speed drives. This is mainly due to their unique capabilities of operation. VRMs' are now finding increasing use in adjustable speed drives because of the following features and advantages:

- This motor is simple in construction with no winding on rotor and simple concentrated coils on stator.

- It can run successfully at high speeds (about 2 x 105 rpm) because of no winding on rotor and rugged rotor construction.
- Stator windings can be cooled easily and efficiently.
- Because of effective stator cooling, the motor dimensions decrease for a given machine rating.
- As VRM can be operated from unidirectional drive circuits, cost of micro- and power-electronics is reduced.
- VRM operates successfully, though at reduced output, even if one or more phases are out of circuit due to some fault.
- They have capability to run in harsh environments.
- There are no shoot-through faults between the DC buses in the SRM drive converter because each rotor winding is connected in series with converter switching elements.
- Bidirectional currents are not necessary, which facilitates the reduction of the number of power switches in certain applications.
- The open-circuit voltage and short-circuit current at faults are zero or very small.
- The maximum permissible rotor temperature is higher, since there are no permanent magnets.
- There is low rotor inertia and a high torque/inertia ratio.

On account of the favorable features enumerated above, SRM drive is now emerging as an alternative for the general purpose adjustable speed drives. SRM can now compete with adjustable speed dc and induction motor drives.

1.2 Drawbacks

SRM must always be electronically commutated and thus cannot run directly from a dc bus or an ac line. The SRM comes with a few disadvantages among which torque ripple and acoustic noise are the most critical. The double saliency construction and the discrete nature of torque production by the independent phases lead to higher torque ripple compared with other machines. The higher torque ripple also causes the ripple current in the DC supply to be quite large, necessitating a large filter capacitor. The

doubly salient structure of the SRM also causes higher acoustic noise compared with other machines. The main source of acoustic noise is the radial magnetic force induced resonant vibration with the circumferential mode shapes of the stator.

The absence of permanent magnets imposes the burden of excitation on the stator windings and converter, which increases the converter KVA requirement.

1.3 Applications [4-9]:

The simple motor structure and inexpensive power electronic requirement have made the SRM an attractive alternative to both AC and DC machines in adjustable-speed drives. An example of SRM application is in heating, ventilation, and air conditioning (HVAC).

SRM drives have great potential for use within the various aspects of conventional automobiles. Example applications of SRMs within an automobile are for the electric power steering and antilock braking systems. The SRM drive is also a strong candidate for the main propulsion drive of an electric or hybrid vehicle. The wide constant power range of SRM drives is especially suitable for such applications

The SRM is also suitable for many industrial and manufacturing applications. For example, high-speed adjustable-speed pumping of fluids for a variety of petrochemical, food processing, and other applications can be done with large horsepower SRM drives.

1.4 Literature Review

Krishnan, R [1] elaborately discussed the Switched Reluctance Motor Drives in detail. This book provides state-of-the art knowledge of SRMs, power converters, and their use with both sensor-based and sensorless controllers. This book presents a unified view of the machine and its drive system from all of its system and subsystem aspects. With a careful balance of theory and implementation, the author develops the analysis and design of SRMs from first principles, introduces a wide variety of power converters available for driving the SRM, and systematically presents both low and high performance controllers. The material in this book is a collection of numerous IEEE papers published up to date, and the author himself has published nearly 100papers in this area.

Timothy L. Skvarenina [2], in his handbook covered the very wide range of topics that comprise the subject of power electronics blending many of the traditional

topics with the new and innovative technologies that are at the leading edge of advances being made in this subject. Emphasis has been placed on the practical application of the technologies discussed to enhance the value of the book to the reader and to enable a clearer understanding of the material. Switched reluctance machines chapter has been described briefly covering all the topics. Bhimbra.P.S [3], in his book had given a concise introduction to SR Machines. This material gives a good idea about the machine for the beginners.

Switched Reluctance Motor is being used for many applications because of its simple construction and ruggedness. A lot of research is going on to improve the performance of SRM. References [4-9] deal with SRM applications such as vaccum cleaner, Steering Vane Control on the Landing Craft Air Cushion (LCAC) Hovercraft, blower, spindle motor etc.

Slobodan Vukosavic and Victor R. Stefanovic in their publication [10] titled, "SRM Inverter Topologies: A Comparative Evaluation," ", bring out clearly the working of each of the topologies for SRM inverter. Also, several inverter power circuits that are suitable for SRM Drives are analyzed and compared with each other.

A.V.Radun in his publication [11] titled, "Design considerations for the Switched Reluctance Motor", had presented the analytical design equations to predict the performance and to guide the design of the SRM. The use of these equations to trade off different SRM attributes is discussed. [12], [13] also give a good design analysis.

References [14-27] deal with the modeling, simulation and control of SRM. Liuchen Chang [16], Syed A. Hossain and Iqbal Husain [24], Suying Zhou, Hui Lin [27] have modeled the SRM. The advanced modeling methods were given in these papers. F. Soares, P. J. Costa Branco [14], H. Chen, J. Jiang, D.Zhang and S. Sun[19], Chong- Chul Kim, Jin Hur, Dong- Seok Hyun [21], had given the different simulation techniques for simulation of SRM in MATLAB. The simulations were done in both Simulink and also using m-file. J. Mahdavi, G. Suresh, B. Fahimi, M. Ehsani [17], O. Ichinokura, T. Onda, et al. [18] , gave the simulation models in PSPICE. I. El-Samahy, M. I. Marei and E. F. El-Saadany [25] gave the simulation model of SRM in EMTDC/PSCAD Software.

Hamid Ehsan Akhter, Virendra K. Sharma, et al. [15], Hamid Ehsan Akhter, Virendra K. Sharma et al. [23] and Mohamed N. Abdul Kadir, Abdul Halim Mohd.

Yatim [26] give the significance of excitation angles. The performance analysis of the SRM is done. [15] determines the optimum turn off angle for rated torque. [26] determines the optimum switching angles for maximum efficiency operation. Tauter T. Borges, Darizon A. de Andrade, et. al [20] gives the concept on current control of SRM. Phop Chancharoensook, Muhammed F Rahman [22] used look-up tables in the simulation of the SRM model. Lookup tables are used for the determination of current and torque.

References [28-31] deal with fuzzy logic control of SRM. Silverio Bolognani and Mauro ZigliottoFuzzy [28], deals with the fuzzy logic control of an SRM drive. The fundamentals of the switched reluctance motor using fuzzy logic are illustrated, pointing the aspects related to the speed control. A fuzzy logic controller (FLC) of the motor speed is then designed and simulated. [32,33] deal with torque ripple minimization.

References [34-40] give different hardware implementation techniques. Virendra Kumar Sharma, Bhim Singh, S.S. Murthy [34], developed an analog scheme for speed control of switched reluctance motor. The scheme is simple, cost effective and is useful for low rating applications. The power and control circuits of the SRM drive were designed and developed. B.K.Bose et al. [35] describes a microcomputer based four quadrant control system of an SRM. The angle controller is designed using dedicated digital hardware. Intel 8751 single chip microcomputer is also used for the implementation.

References [41-44] give the application notes for DSP based applications of SRM. These documents deal with solutions to control a switched reluctance motor using the DSP kits. They give cost-effective design of intelligent controllers for switched reluctance motors. Speed control algorithms were given which allow the Switched Reluctance Motor drive to reach high efficiency, smooth operation, very good dynamic behavior, very high speed and low acoustical noise. These articles also present some mechanical position sensorless algorithms in order to reduce the overall system cost and to enhance the drive reliability.

1.5 Organization of the Report:

CHAPTER II: This chapter focuses on the constructional details, basic principles, basic design considerations and control parameters.

CHAPTER III: This chapter includes the modeling approaches, simulation models and the simulation of current and speed control of SRM. Simulations using and without using Simulink block are shown. The simulations are done in MATLAB R2006a version. The simulations are done on a 6/4 pole SRM.

CHAPTER IV: The hardware implementation is presented in this chapter. Various circuits' description like power circuit, power amplification and isolation circuits, etc are discussed. Interfacing circuits are presented. The starting problem of SRM is discussed and an algorithm to solve it is given. Software implementation is explained through flowcharts.

CHAPTER V: This chapter has the results of the simulation for current control and speed control of the SRM. The simulations are done for step change in load and reference. Fuzzy controller was also used as speed controller. Performance of SRM is also investigated for different switching angles. The impact of turn off and turn on angles is studied. The optimum turn off angle for a particular load is determined. The affect of turn-on angle on speed response for a particular load for different turn-on angles is also determined.

CHAPTER VI: This chapter presents the conclusion of this thesis and scope for future work in this area.

1.6 Conclusion:

Different modeling approaches and simulation models of SRM are studied. Analytical modeling approach of SRM is implemented and a simulation model with mathematical evaluation of the inductance is used in the thesis. The speed response of an SRM drive is studied for changes in the load, reference current and speed. Performance investigations on SRM are done by emphasizing on the switching angle control. Hardware implementation of the microcontroller controlled SRM drive is done with a simple converter topology.

2.1 Constructional Details: Switched Reluctance Motor is a doubly-salient, singly-excited reluctance machine with independent phase windings on the stator, usually made of magnetic steel laminations. The rotor is a simple stack of laminations, without any windings or magnets. The cross-sectional diagram of a three-phase, 6/4 SRM is shown in Fig. 2.1. The stator windings on diametrically opposite poles are connected either in series or in parallel to form one phase of the motor. When a stator phase is energized, the most adjacent rotor pole-pair is attracted toward the energized stator to minimize the reluctance of the magnetic path. Therefore, it is possible to develop constant torque in either direction of rotation by energizing consecutive phases in succession.

The aligned position of a phase is defined to be the situation when the stator and rotor poles of the phase are perfectly aligned with each other attaining the minimum reluctance position. The unsaturated phase inductance is maximum at this position. The phase inductance decreases gradually as the rotor poles move away from the aligned position in either direction. When the rotor poles are symmetrically misaligned with the stator poles of a phase, the position is said to be the unaligned position. The phase has the minimum inductance in this position.

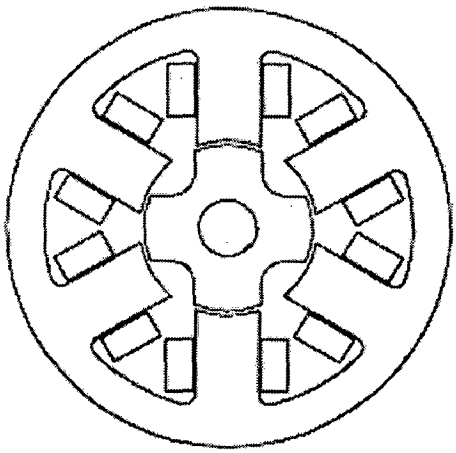

FIGURE 2.1 Cross-Section of a 6/4 SRM

Several other combinations of the number of stator and rotor poles exist, such as 8-6, 10-4, 12-8, etc. A 4-2 or a 2-2 configuration is also possible, but they have the disadvantage that, if the stator and rotor poles are aligned exactly, then it would be

impossible to develop a starting torque. The configurations with higher number of stator/rotor pole combinations have less torque ripple and do not have the problem of starting torque.

2.2 Basic Principle of Operation

The rotor of SRM is aligned whenever diametrically opposite stator poles are exited. In a magnetic circuit, the rotating member prefers to come to the minimum reluctance position at the instance of excitation. While two rotor poles are aligned to the two stator poles, another set of rotor poles is out of alignment with respect to a different set of stator poles. Then, this set of stator poles is exited to bring the rotor poles into alignment. Likewise, by sequentially switching the currents into the stator windings, the rotor is rotated. The movement of the rotor, hence the production of torque and power, involves switching of currents into stator windings when there is a variation of reluctance. This switching can be done through a power converter.

The general equation governing the flow of stator current in one phase of an SRM can be written as

$$V_{ph} = iR + \frac{d\lambda}{dt} \tag{2.1}$$

Where V_{ph} is the DC bus voltage, i is the instantaneous phase current, R is the winding resistance, and λ is the flux linking the coil. The SRM is always driven into saturation to maximize the utilization of the magnetic circuit, and, hence, the flux-linkage λ is a nonlinear function of stator current and rotor position

$$\lambda = \lambda(i, \theta) \tag{2.2}$$

The electromagnetic profile of an SRM is defined by the λ–i–θ magnetization characteristics shown in figure 2.2.

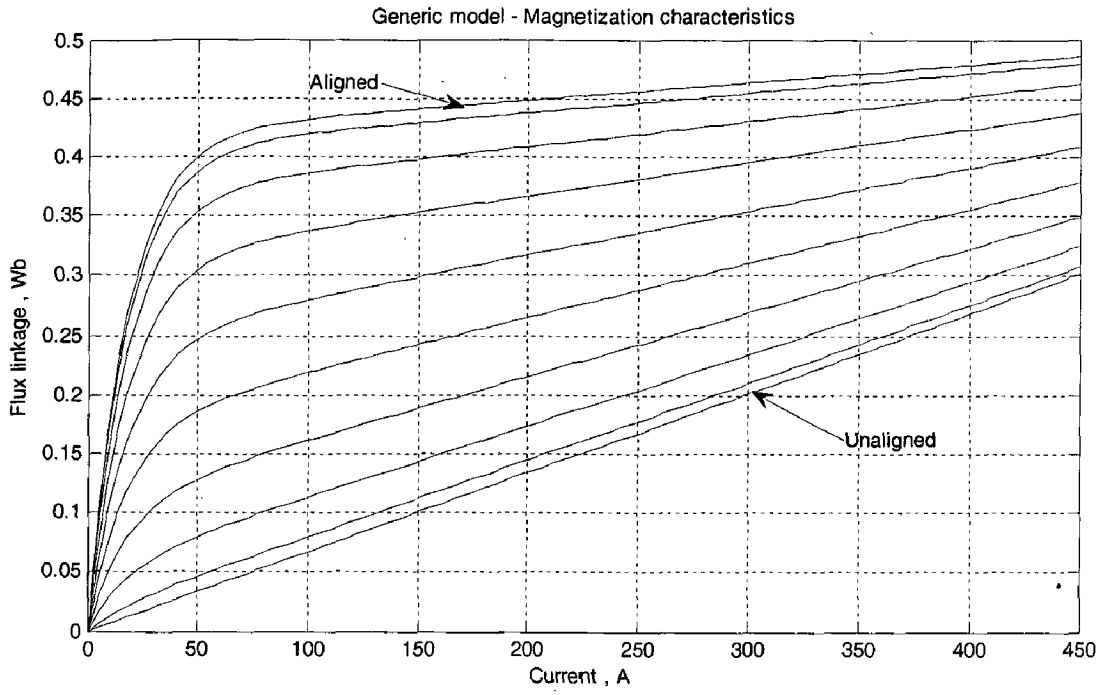

FIGURE 2.2 Flux–angle–current characteristics of a four-phase SRM.

The three dimensional relationship [1] can be seen among current, flux linkage and rotor position. Figure 2.3 shows the variation of flux with rotor position for constant current, I_{se}. And similarly, for constant flux linkage (λ_{se}), the current vs. rotor position is extracted as shown in figure 2.4.

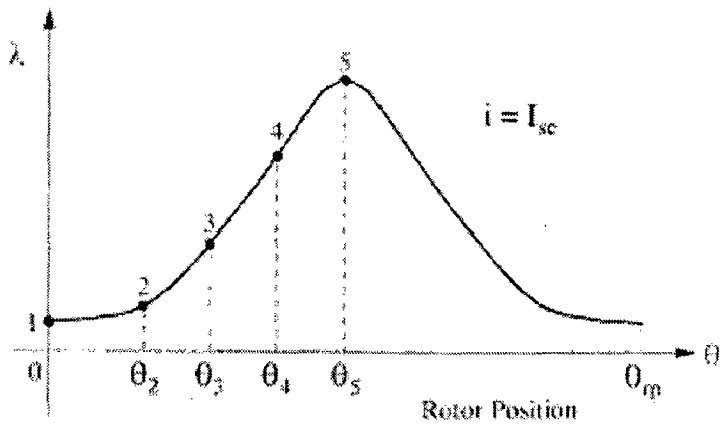

FIGURE 2.3 Flux linkage vs. rotor position at constant current I_{se}.

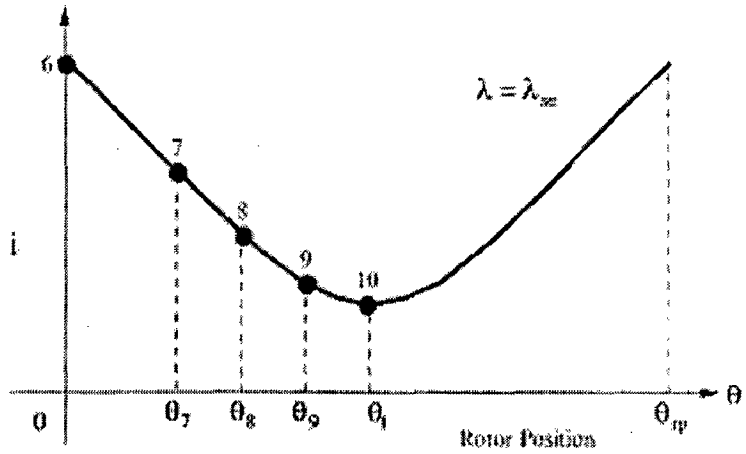

FIGURE 2.4 Phase current vs. rotor position at constant flux linkages.

The stator phase voltage can be expressed as

$$V_{ph} = iR + \frac{d\lambda}{di}\frac{di}{dt} + \frac{d\lambda}{d\theta}\frac{d\theta}{dt} \tag{2.3}$$

Assuming magnetic linearity (where $\lambda = L(\theta).\ i$), the voltage expression can be simplified as

$$V_{ph} = iR + L(\theta)\frac{di}{dt} + i\frac{dL(\theta)}{dt}\omega \tag{2.4}$$

where $\omega = d\theta/dt$ is the rotor angular speed. The last term in the above equation contains the product of two variables i and ω, from this it can be inferred that an SRM is a non-linear machine.

2.3 Torque Production

Torque is produced in the SRM by the tendency of the rotor to attain the minimum reluctance position when a stator phase is excited. The torque expression can be derived from co-energy [1], [2].

When magnetic saturation is neglected, the instantaneous phase torque expression becomes

$$T_{ph}(\theta, i) = \frac{1}{2} i^2 \frac{dL(\theta)}{d\theta} \tag{2.5}$$

The total instantaneous torque of the machine is given by the sum of the individual phase torques.

$$T_{inst}(\theta, i) = \sum_{phases} T_{ph}(\theta, i) \tag{2.6}$$

The phase current needs to be synchronized with the rotor position for effective torque production. The torque expression also implies that the direction of current is immaterial in torque production. The optimum performance of the drive system depends on the appropriate positioning of phase currents relative to the rotor angular position. Therefore, a rotor position transducer is essential to provide the position feedback signal to the controller.

2.4 CONTROL PRINCIPLE:

Given the inductance profile shown in Figure 2.5 for motoring operation, the phase windings are excited at the onset of increasing inductance. The torque production for motoring and regeneration is also shown in Figure 2.5

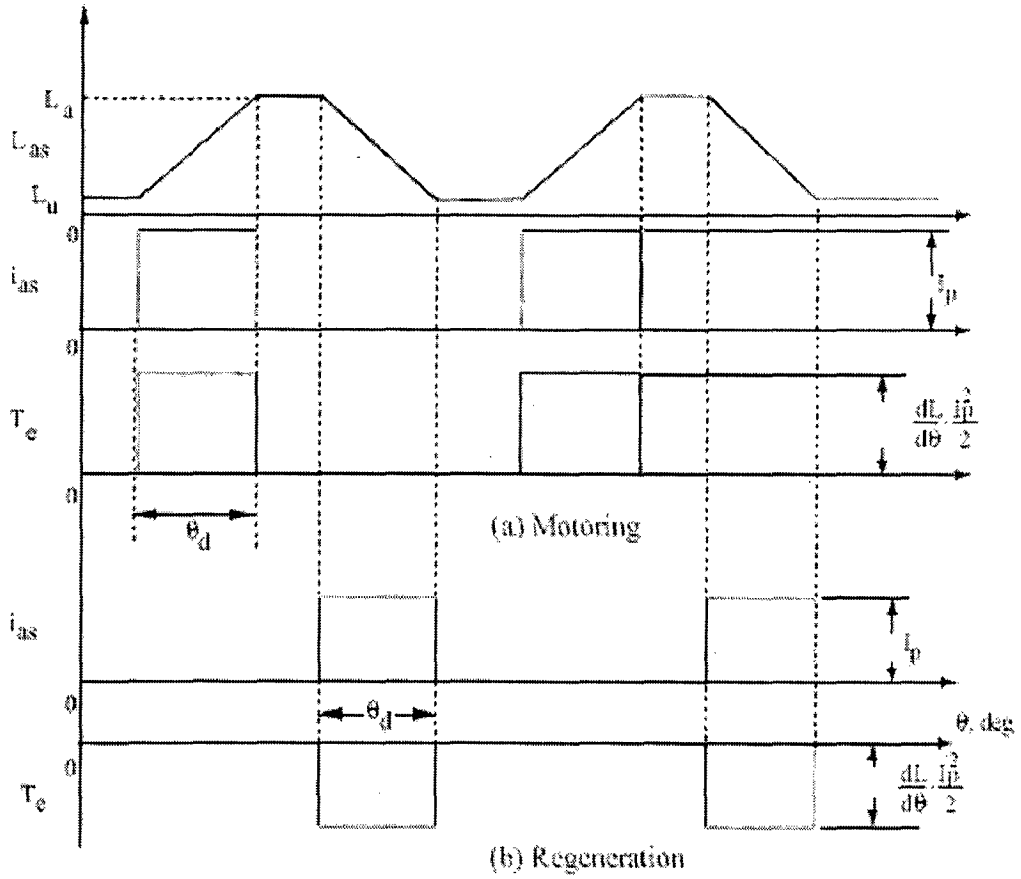

Fig. 2.5 Motoring and regenerative actions of SRM

The torques shown is for only one phase. An average torque will result due to the combined instantaneous values of electromagnetic torque pulses of all machine phases. The machine produces discrete pulses of torque and, by proper design of overlapping inductance profile, it is possible to produce a continuous torque. In actual practice, it will

result in reduced power density of the machine and increased complexity of control of the SRM drive.

2.5 Salient Design Considerations

The fundamental design rules governing the choice of phase numbers, pole numbers, and pole arcs of SRM are discussed in detail by A.V.Radun [11]. From a designer's point of view, the objectives are to minimize the core losses, to have good starting capability, to minimize the unwanted effects due to varying flux distributions and saturation, and to eliminate mutual coupling. The choice of the number of phases and poles is open, but a number of factors need to be evaluated prior to making a selection.

The fundamental switching frequency is given by

$$f = \frac{N}{60} N_r \tag{2.7}$$

where N is the motor speed in rev/m and Nr is the number of rotor poles. The "step angle" or "stroke" of a m-phase SRM is given by

$$\text{Step angle}, \varepsilon = \frac{360}{m.N_r} \tag{2.8}$$

The stoke angle is an important design parameter related to the control frequency per rotor revolution.

2.6 Control of SRM

The control parameters of SRM are the turn-on angle, turn-off angle and the dc link voltage. The switching angles are controlled through a power converter which is fed from a fixed dc link voltage. The torque developed in an SRM is independent of the direction of current flow. Therefore, unipolar converters are sufficient to serve as the power converter for the SRM, unlike induction motors or synchronous motors, which require bidirectional currents. This unique feature of the SR Motor, together with the fact that the stator phases are electrically isolated from one another, has generated a wide variety of power circuit configurations. The type of converter required for a particular SRM drive is intimately related to motor construction and the number of phases. The choice also depends on the specific application.

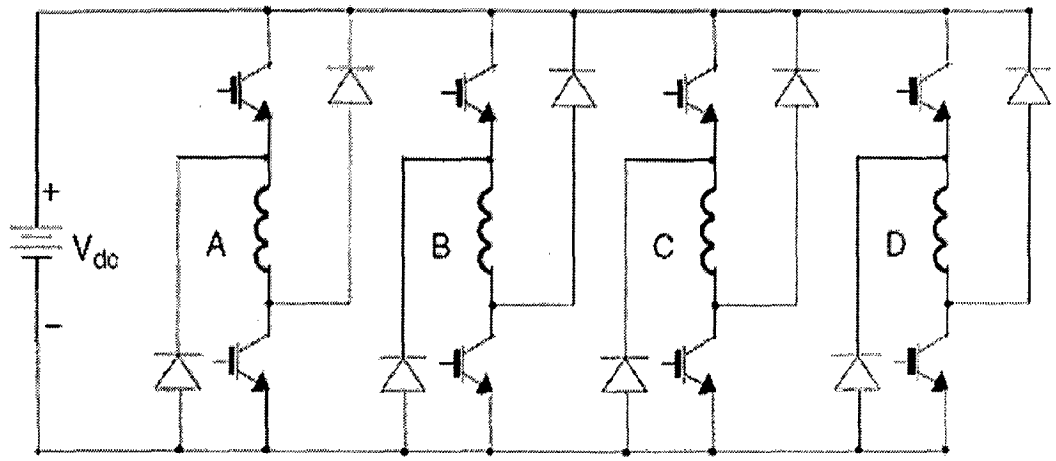

Fig. 2.6 Basic Bridge converter circuit for the SRM

A brief study of all the converter topologies is discussed in [10] and in detail in [1]. The most flexible and the most versatile four-quadrant SRM converter is the bridge converter shown in Fig. 2.6, which requires two switches and two diodes per phase. During the magnetizing period, both the switches are turned on and the energy is transferred from the source to the motor. Chopping or PWM, if necessary can be accomplished by switching either or both the switches during the conduction period according to the control strategy. At commutation both switches are turned off and the motor phase is quickly de-fluxed through the freewheeling diodes. The advantage of this converter is the independent control of each phase, which is particularly important when phase overlap is desired. The only disadvantage is the requirement of two switches per phase. This converter is especially suitable for high voltage, high power drives.

2.7 Conclusion

In this chapter, the basic theory regarding SRM is presented. The constructional details and basic design considerations are given concisely. The principle of operation and the torque production concepts are presented with the help of simple figures for easy understanding.

3.1 Introduction

The simulation of SRM drive system is complex than ac and dc motor drives because of its nonlinear operation. This nonlinearity is due to dependence of phase flux linkages on both rotor position and current. For separately excited dc machines and synchronous machines, the system can be made linear by making either armature or field mmf constant. This is not possible in the case of SRM because of single source of excitation.

A dynamic simulation of the drive system enables verification of the analytical designs and ability of the motor drive system to match the load torque over its entire speed range both in its steady state and during transients. With such verification, time and cost of product development are minimized by avoiding a trial-and-error approach to prototype construction that may lead to repetitive testing and redesign until specifications are met. Such a trial-and-error process in design is very costly and time consuming. The main benefits to be achieved are

- Gain of time for the simulation development.
- Choice of several techniques of numeric resolution;
- Several available libraries for different domains as, for example, fuzzy-logic control, neural networks, and signal processing.

Simulation of the drive system requires models for the SRM drive subsystems and their interconnections. This chapter contains the subsystem models and their derivation and a procedure for simulation of the drive system.

Modeling of Switched Reluctance Motors [1]

A general schematic of a drive system is shown in figure 3.1. The block diagram is confined to controller section and only essential elements of the drive system are considered to generalize the model. Given a speed command, the current reference for a particular rotor position is found from the controller. The current reference is compared with the phase currents and the error is given to converter through a controller, on which the phases are excited. The machine equations, the input voltages, and the machine characteristics captured in the three-dimensional relationships are used to determine the

phase currents, air gap torque, rotor speed, and rotor position. With the available computed currents and rotor speed, their respective errors are then found for use in the controller to determine the reference current. The three dimensional relationship is used during the modeling of SRM.

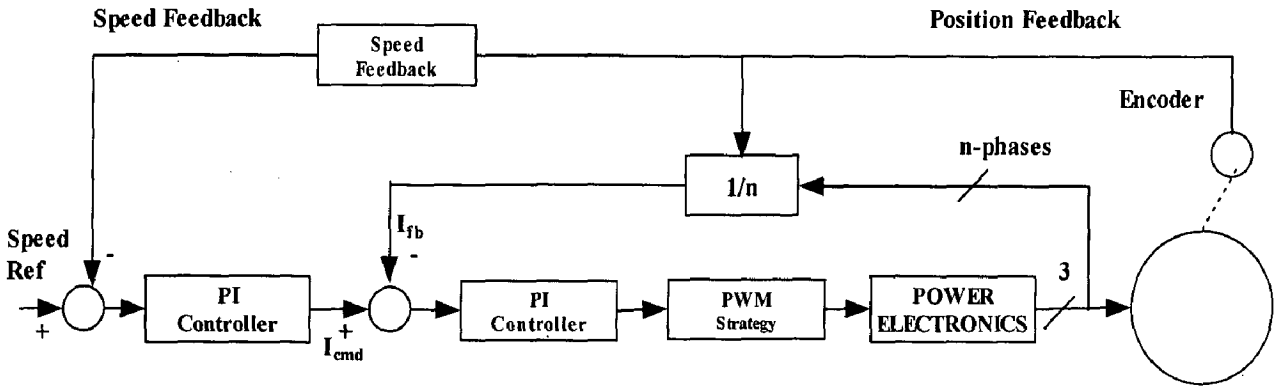

Fig. 3.1 Block diagram to show the speed control of SRM

3.2 Modeling Approaches

There are two approaches to establish a model of SRM: analytical approach based on generalized electrical machine theory and finite element approach. With the analytical method, the entire SRM geometry is divided into small magnetic segments subject to non-linear magnetic characteristics. Using the magnetic equivalent circuit principles, the flux and flux linkage of the stator windings can be calculated for certain stator current excitations. The self and mutual inductances of an SRM can then be determined and used in the differential equations describing the SRM. This analytical model offers fast waveforms and performance computations, however is inaccurate due to the complicated shapes of the SRM magnetic circuit and the non-linear characteristics of the magnetic materials.

Analytical calculations of flux linkages are possible and are easy for aligned positions of SRM. But, it is difficult for unaligned position, because the leakage paths are not known a priori. Finite element analysis techniques are used to estimate the flux linkages. The finite element method (FEM) takes into account the non-linear magnetic property and detailed SRM geometry. Finite element analysis provides more accurate results rather than the magnetic equivalent circuit approaches because it considers a large number of flux paths compared to the magnetic equivalent circuit method.

FEM also have some disadvantages. The calculations involved are complex and time consuming. The relationship of motor output variables to motor dimensions, number of poles, number of turns per phase, excitation current, and current conduction angle is not explicit. Hence, a change in one or many of the motor and control variables requires an entire finite element analysis computation which is either in two or three dimensions. Each set of finite element computations takes a considerable amount of time. The analytical based approach model is used in all the simulations of the work.

3.3 Mathematical Model

A dynamic mathematical model of a SRM is composed of a set of electrical equations for each phase and equations of mechanical system. In a typical m-phase SRM, if mutual inductance is neglected, the machine's voltage equation can be expressed as:

$$v_j = R_j.i_j + \frac{d\lambda_j(i_j,\theta)}{dt}, j = 1,...,m, \tag{3.1}$$

$$\text{i.e, } \frac{d\lambda_j(i_j,\theta_j)}{dt} = v_j - R_j.i_j, j = 1,...,m, \tag{3.2}$$

where v_j is the terminal voltage of phase j, i_j is phase current, R_j is phase winding resistance, λ_j is the flux linkage and θ_j is rotor position. The flux linkage is a function of current and rotor position.

The mechanical dynamic equations can be expressed as:

$$\frac{d\theta}{dt} = \omega, \tag{3.3}$$

and

$$\sum_{j=1}^{m} T_j(i_j,\theta) - T_l = J.\frac{d\omega}{dt} + B.\omega, \tag{3.4}$$

where T_j is the phase torque and T_l is the load torque. J and B represent the moment of Inertia and coefficient of friction, respectively.

The speed equation can be rearranged as,

$$\frac{d\omega}{dt} = \frac{1}{J}\left(\sum_{j=1}^{m} T_j(i_j,\theta) - T_l - B.\omega\right) \tag{3.5}$$

Equations (3.2), (3.3) and (3.5) form the dynamic model.

From section 2.2.2, we know that the phase torque is given by equation (2.6)

$$T_j(i_j,\theta) = \frac{1}{2} i_j^{\,2} \frac{dL_j(\theta)}{d\theta}$$

3.4 Simulation Models

Simulation modeling of SRM is complex because of its nonlinearity and its three dimensional characteristics between flux, current and rotor position. The inductance profile is not linear. There are many simulation models of SRM. Some of them are:

Look-up tables [22]: Look up tables are used for the determination of current and torque for different rotor angles. This is done in Simulink block of MATLAB shown in Fig 3.3.

Fourier series [15]: Fourier series can be used to model the inductance profile . In this, the inductance value is determined in terms of the Fourier coefficients with rotor angle.

Mathematical Evaluation [14]: In this method, the inductance value is determined from the maximum and minimum inductance values, and the stator and rotor pole arcs. Inductance value corresponding to a particular rotor angle is determined from its profile using mathematical calculations. This method is used in the thesis for the simulation of SRM without using Simulink block of SRM.

3.5 Simulation of SRM drive using MATLAB

All the simulations are carried out in R2006a version of MATLAB. All the simulations are done on 3- phase 6/4 pole switched reluctance motor.

3.5.1 Simulink block of SRM

A modeled Switched Reluctance Motor is available in the Simulink library of MATLAB. Depending on the motor configuration specified by the Type parameter, this block models different configurations such as:

- a three-phase Switched Reluctance Motor having 6 stator poles and 4 rotor poles.
- a four-phase Switched Reluctance Motor having 8 stator poles and 6 rotor poles.
- a five-phase Switched Reluctance Motor having 10 stator poles and 8 rotor poles.

A generic model or a specific model can be used. The generic model is characterized by the aligned and unaligned inductances, the saturated aligned inductance, the maximum current, and the maximum flux linkage. The specific model is characterized by the magnetization characteristic given as a table of flux linkage in

function of the rotor position and the stator current. Figure 3.2 shows the block for a three-phase Switched Reluctance Motor and the block parameters corresponding to it. The internal model is shown in figure 3.3 which is modelled by considering the dynamic equation and the look up tables for the required magnetization and torque-current characteristics.

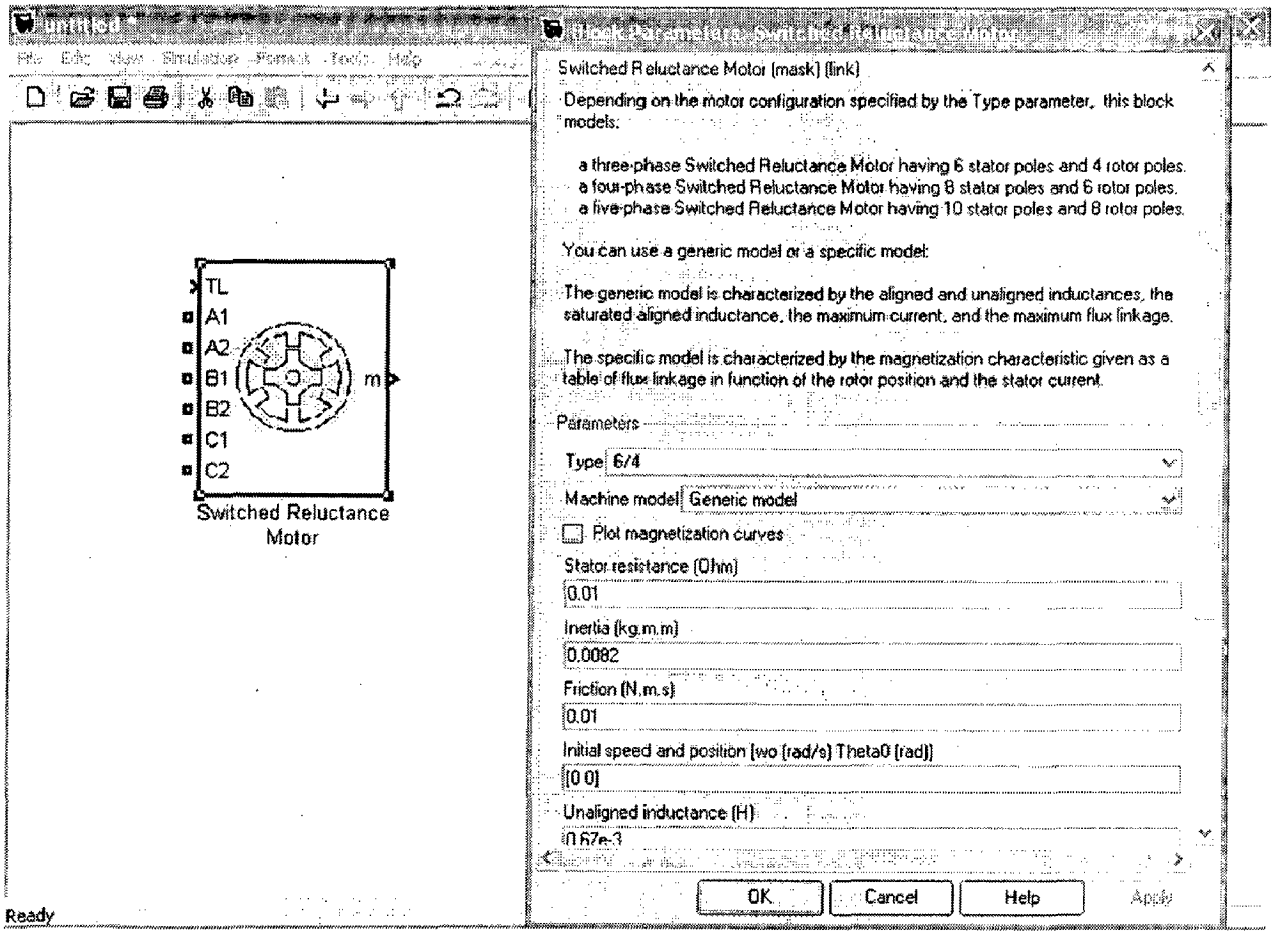

Fig. 3.2 Simulink block for a three-phase Switched Reluctance Motor and the block parameters

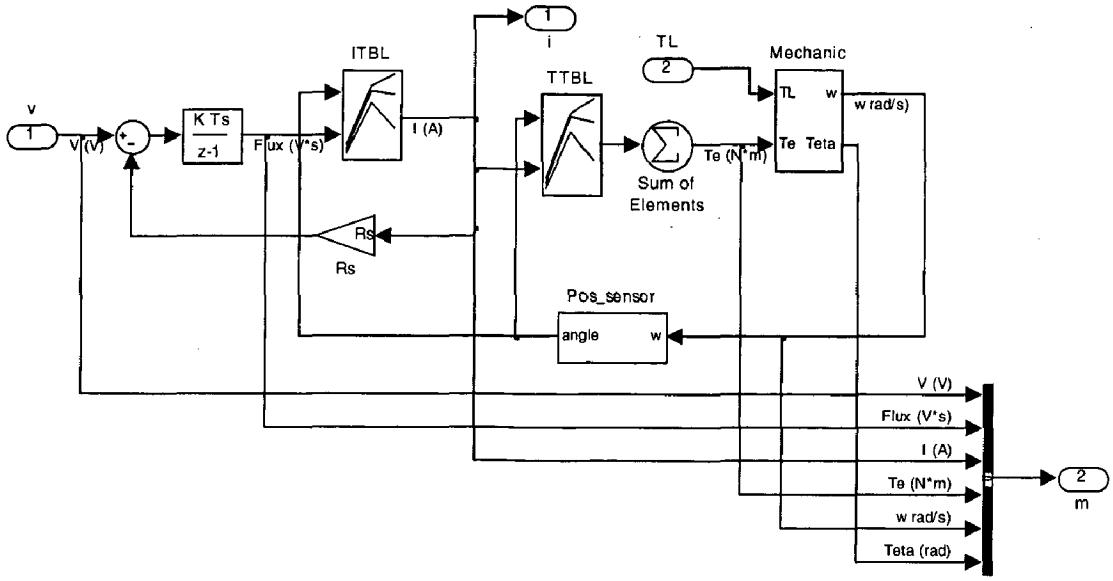

Fig. 3.3 Subsystem showing the internal simulation model of one phase of SRM

3.5.2 Simulation of current controlled 6/4 SRM drive

Simulation model of a current controlled SRM drive is shown in figure 3.4. The blocks in the model are the power converter, SRM block, position sensor block, relay etc. The current error is given to a relay which controls the gates of the power converter. A simple power converter with one switch per phase is used. Figure 3.5 shows the model of the converter of one phase with the winding terminal coming out. The reference current is multiplied either by 1 or 0 depending upon the rotor position. If the rotor position is between the turn on and turn off angle then the reference current is multiplied by 1 else with 0. The converter is connected to the phase windings of the SRM block. The block then simulates the switched reluctance motor for the corresponding excitation. The variables such as flux linkages, phase currents, phase torques, phase voltages, speed can be obtained from the block. The speed obtained is given as feedback through a position sensor. The angular position is determined from the speed and the current command to be fired is determined for all the phases based on it. All the phases have a similar model except the phase inductances are displaced by an angle θs, which is given by

$$\theta_s = 360\left(\frac{1}{N_r} - \frac{1}{N_s}\right) \quad \text{degree} \qquad (3.6)$$

where Ns and Nr are the number of stator and rotor poles. For a 6/4 SRM, $\theta_s=30^o$.

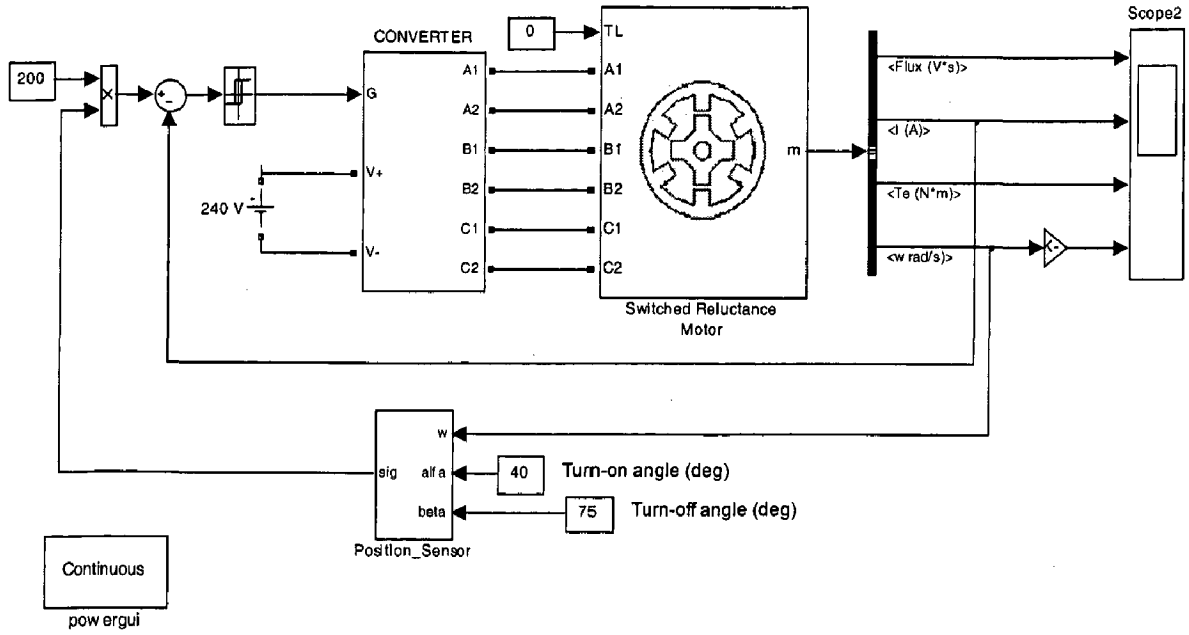

Fig. 3.4 Simulink model of a Current Controlled SRM Drive

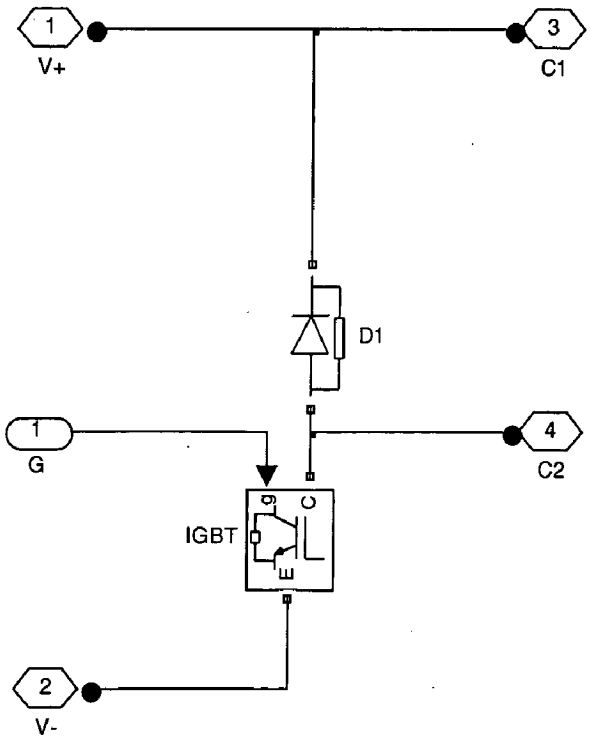

Fig. 3.5 Simulink model of one phase of the power converter

Simulation of current controlled SRM without Simulink block

The simulation diagram used for the SRM model is shown in figure 3.6. A strong aspect of the SRM simulation using Simulink is the use of conventional blocks allowing easier understanding of the programmer's structure. The parameters of the SRM model are initialized through a program and are made to be available in the work space. The models of all the phases are same except the phase angles displaced by an angle θs. The subsystem of Phase I is shown in figure 3.7. Each phase contains four blocks, each one associated with a specific Matlab function. They are the following.

Switch: The inputs to this function are the current chopping controller output and the rotor angle, and the output is the phase voltage. Switch permits to assure the power converter commutations based on turn on, turn off angles.

Inductance: Inductance block computes the current on the respective phase inductance according to rotor position and phase flux. The inductance is estimated based on the rotor position by using the linear equations. From the known flux and inductance, current is determined.

Torque: This block computes the torque produced in the phase according to the rotor position and the phase current.

Modulo pi/2: Each phase inductance has a periodicity of 360/ Nr degrees. Hence, the rotor position angle which is coming from the mechanical equation is transformed to modulo 360/ Nr. For a 6/4 SRM, the periodicity is 90°.

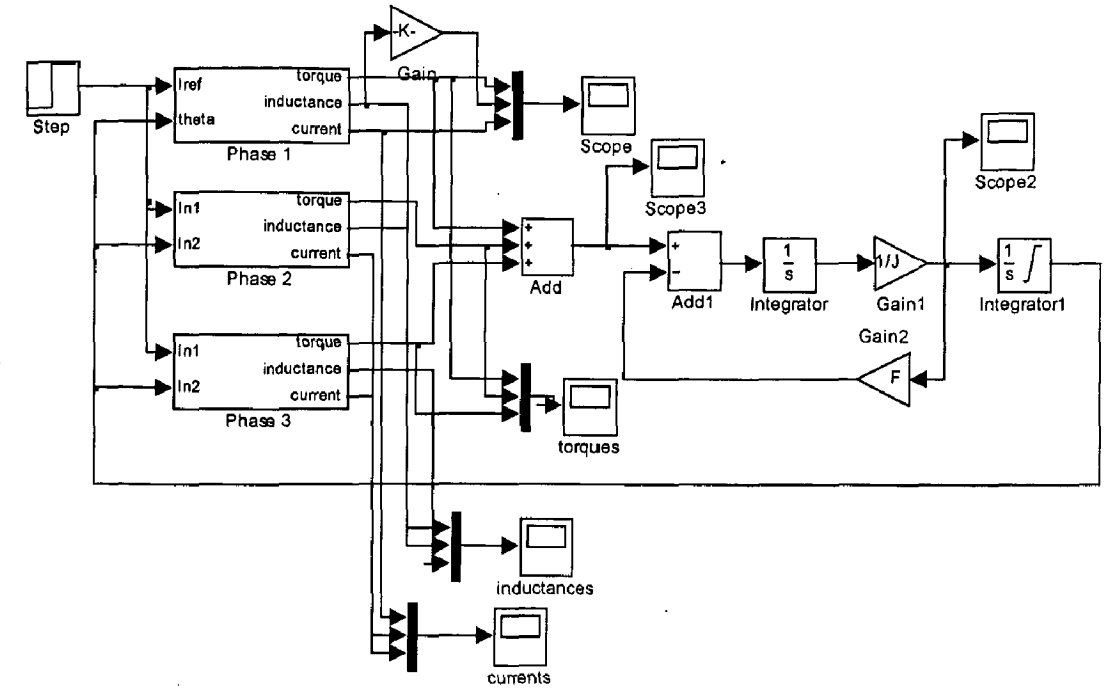

Fig 3.6 Simulink diagram of SRM model

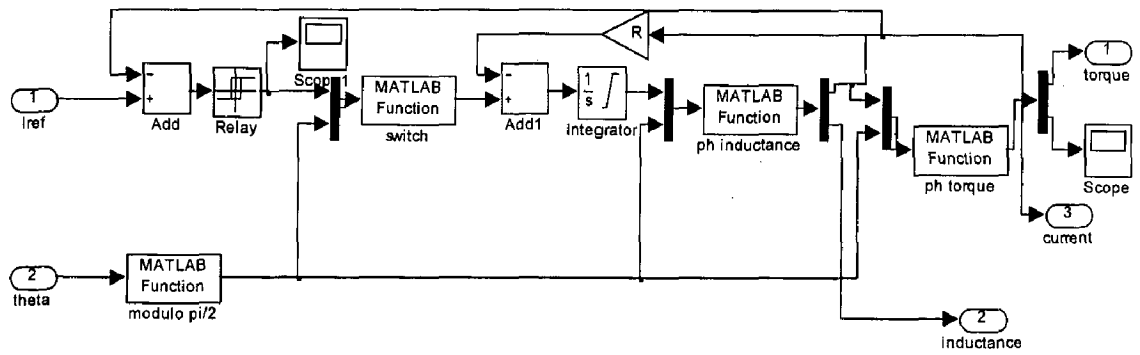

Fig. 3.7 Internal Block phase I

3.5.3 Simulation of speed control of a 6/4 SRM drive

The simulation model of the speed control of a 6/4 SRM drive is shown in figure 3.8. It consists of outer speed loop and inner current loop. The block diagram showing the speed control of SRM is given in figure 3.1.The reference speed compared with the rotor speed is the speed error. The speed error signal is processed through a proportional plus integral speed controller to yield the reference current. This reference current is compared with the motor currents and the errors are used to determine the switching of the phase and the

main switches of the power converter. Then, the voltages are applied to the respective windings based on their position information obtained from position sensor.

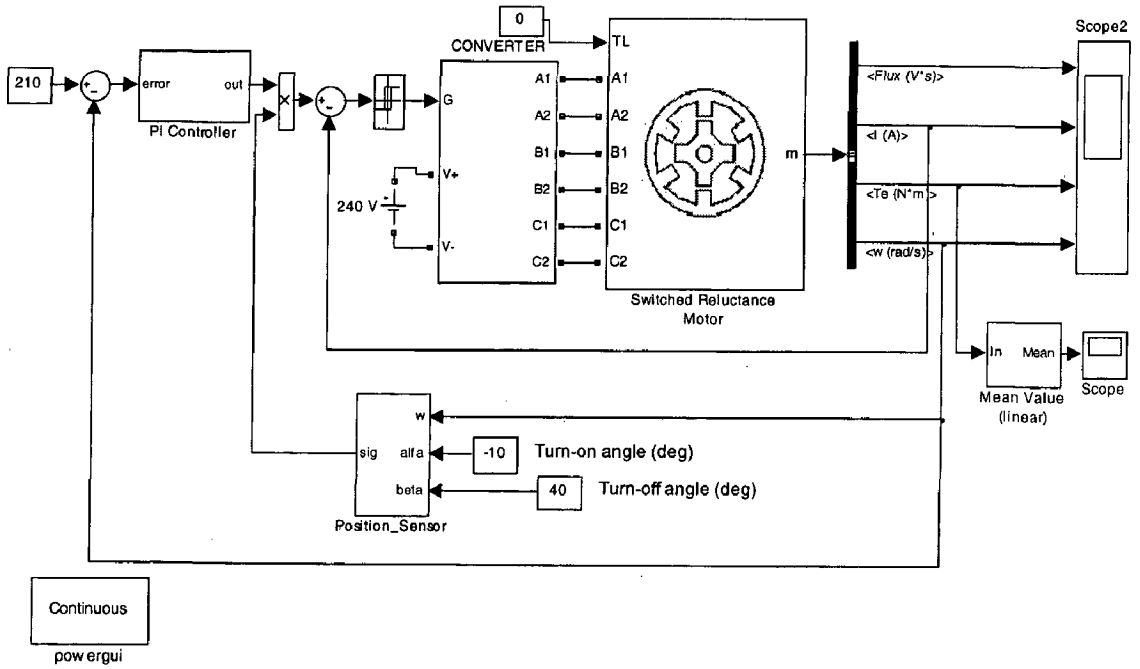

Fig 3.8 Simulink model showing the double closed loop speed control of SRM Drive

Simulation of speed control of a 6/4 SRM drive without Simulink block

Figure 3.9 shows the speed control of a 6/4 SRM drive without Simulink block.

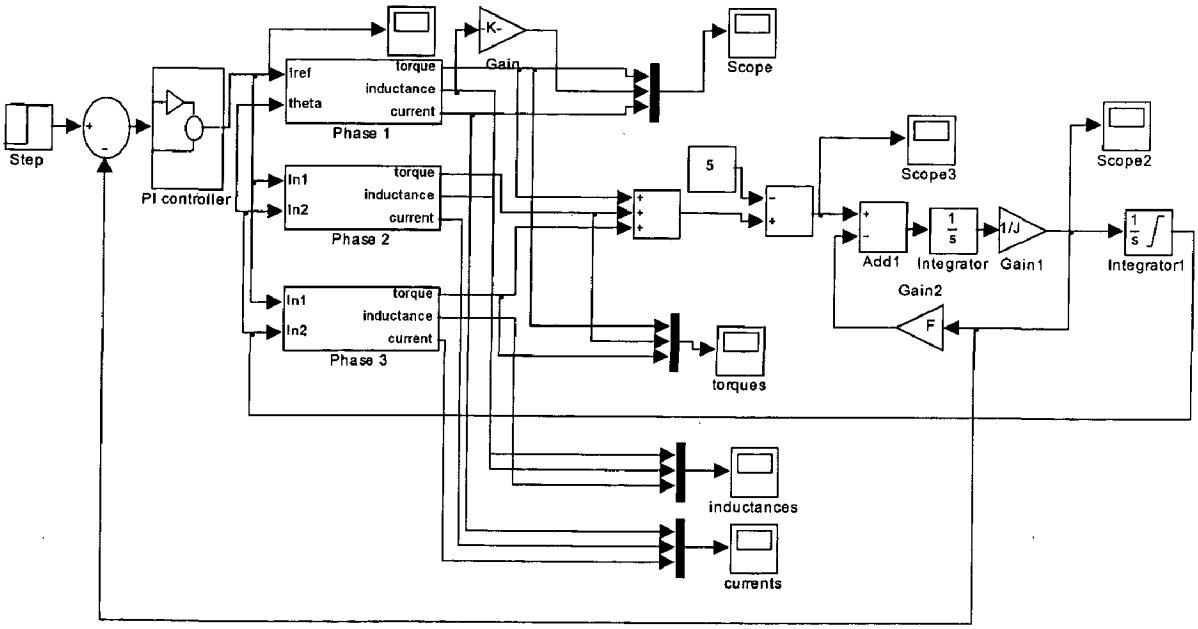

Fig 3.9 Simulink model showing the speed control of SRM Drive

Simulation of speed control of a 6/4 SRM drive using Fuzzy Logic

The controller used in the last section is the PI controller. Due to the various benefits that the fuzzy logic has over conventional controllers, a Fuzzy controller is placed to see the performance of the speed controller. Application of Fuzzy logic to SRM is presented well in [29-31]. The block diagram showing fuzzy speed controller and its modules is given in figure 3.10.

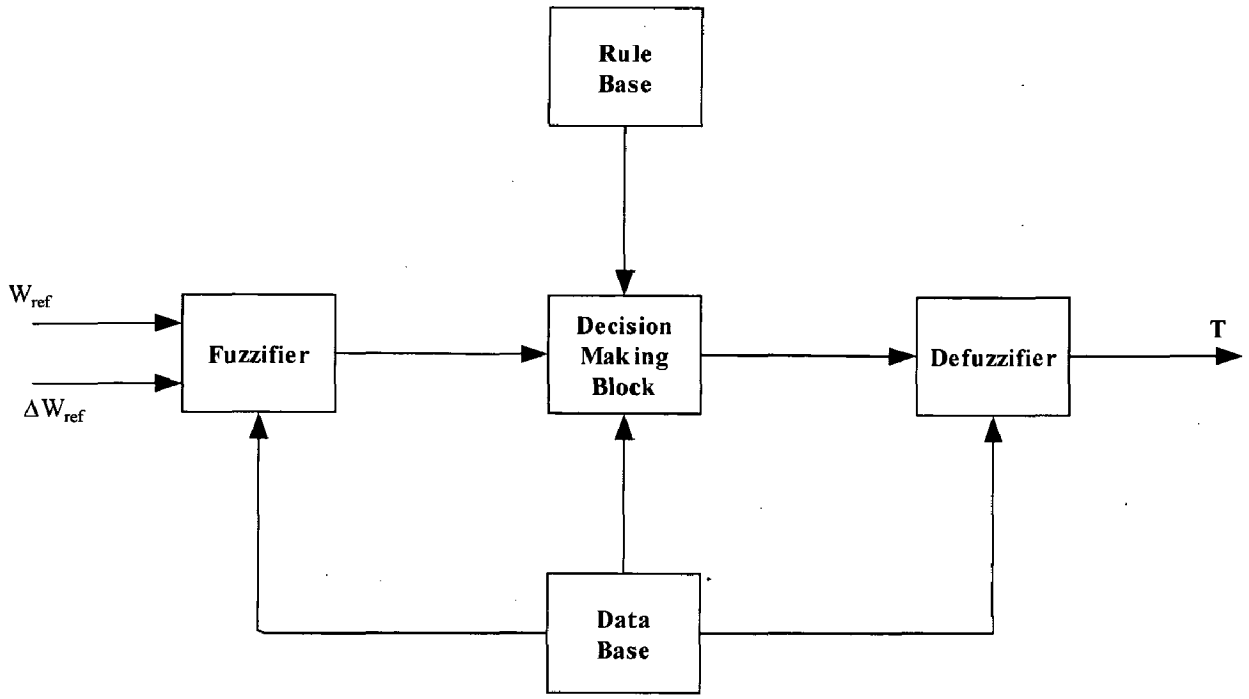

Fig. 3.10 Block diagram showing fuzzy speed controller and its modules

Mamdani method is used and fuzzy centroid algorithm is used for defuzzification. The membership functions for the two inputs and output is shown in figure 3.11 and the rule base in figure 3.12.

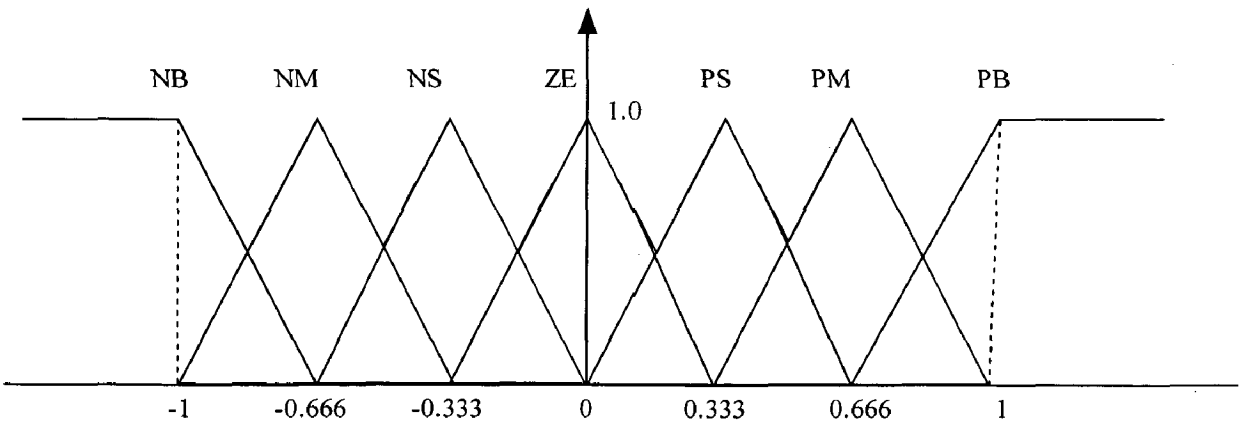

Fig. 3.11 Memberships of the input and output variables

		E						
		NB	**NM**	**NS**	**ZE**	**PS**	**PM**	**PB**
ΔE	**NB**	NB	NB	NM	NM	NS	NS	ZE
	NM	NB	NB	NM	NS	NS	ZE	PS
	NS	NB	NB	NS	NS	ZE	PS	PM
	ZE	NB	NM	NS	ZE	PS	PM	PB
	PS	NM	NS	ZE	PS	PS	PB	PB
	PM	NS	ZE	PS	PS	PM	PB	PB
	PB	ZE	PS	PS	PM	PM	PB	PB

Fig. 3.12 Rule base used for the FLC

The Simulink model for the fuzzy controller is shown in figure 3.13. The error rate is determined with the help of a memory block. The scaling variables in the input side are G1 and G2, and the output scaling variable is G_{out}. The Simulink Fuzzy Logic toolbox was used for the implementation.

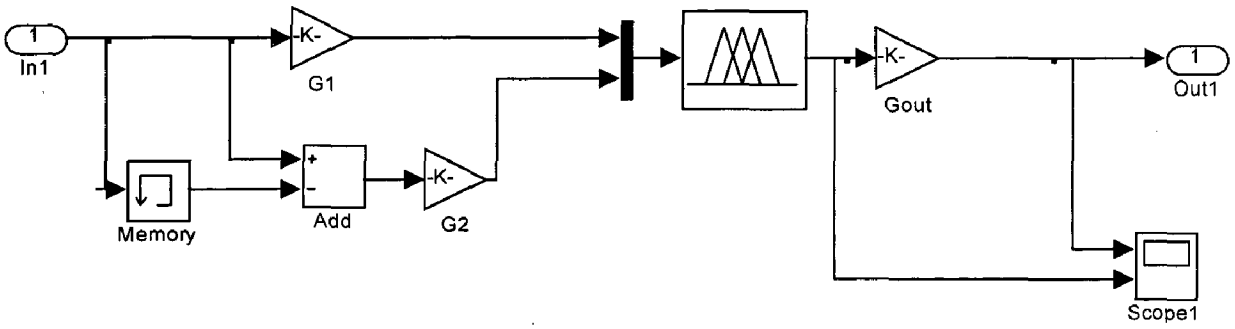

Fig 3.13 Simulink model of the fuzzy logic controller

3.6 Conclusion

Different modeling approaches and simulation models of SRM are presented. A brief description of SRM Simulink block is given. The simulations of SRM drive for current control and speed control are presented. A fuzzy controller was also used along with a PI controller for speed control.

4.1 Introduction

Control signals applied to a power converter can be obtained with the aid of microcomputer software. A reliable, low cost and small sized gate circuit can be realized by using microcomputers. The generation of control signals required to control the SRM is attained by the single chip microcomputer 8031.

Advantages of Microcomputer control:

Microcomputer control of power electronic equipments is commercially attractive because it offers the possibility of improved reliability and increased flexibility particularly in the design of variable speed drives. Some of the advantages of microcomputer control are:

- Significant reduction in controller hardware and manufacturing cost.
- Increased reliability.
- No drift problem and parameter variation effects are non existent.
- No electromagnetic interference problems.
- Universal hardware.
- Sophisticated control possible.
- Fault monitoring data acquisition warning, diagnostic capabilities are possible.

A brief description of Microcontroller is given in Appendix III.

4.2 Hardware implementation:

The hardware implementation is done on a 3-phase, 6/4 pole SRM. The block diagram showing the supply and control of SRM Drive with Microcontroller is shown in figure 4.1. The power inverter circuit is shown in the figure 4.2. The gating signals for the inverter circuit are obtained from the microcontroller.

The phase currents need to be synchronized with rotor position for effective torque production. Also, optimum performance of the drive system depends on the appropriate positioning of the phase currents relative to the rotor angular position. Here, a speed encoder ROD 436 has been used as a rotor position transducer, which provides the position feedback signal to the controller.

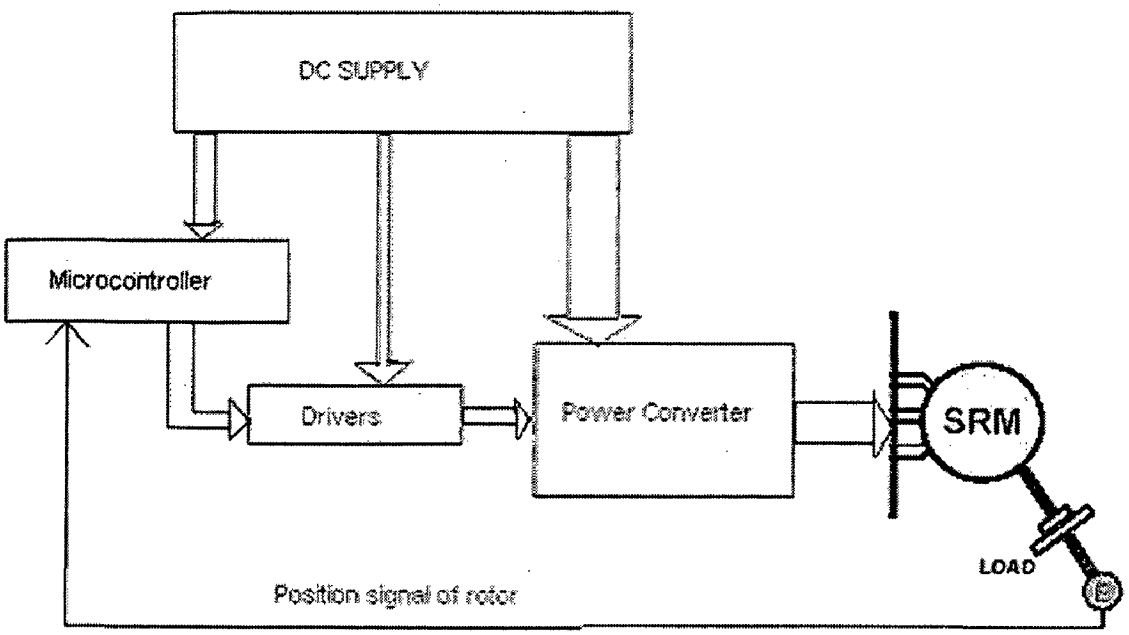

Fig. 4.1 Block diagram to show the supply and control of SRM Drive.

The system hardware can be divided into the following blocks:

- Power circuit
- Pulse amplification and isolation circuits
- Power supplies
- Circuit protection
- Current sensing circuit
- Microcontroller Hardware Kit
- Speed Encoder

Power Circuit:

Fig. 4.2 shows the power circuit of three switch three phase SRM inverter. Each MOSFET switch used in the circuit consists of an inbuilt anti parallel free wheeling diode. No forced commutation circuit is required for MOSFETs because they are self commutated devices (they turn on when the gate signal is high and turn of when the gate signal is low). The winding inductance restricts large di/dt through MOSFETs; hence only turnoff snubber is required for protection. An RCD (resistor, capacitor and diode) turn-off circuit is connected to protect the circuit against high dv/dt and is protected against power voltage by connecting MOV (Metal Oxide Varistor).

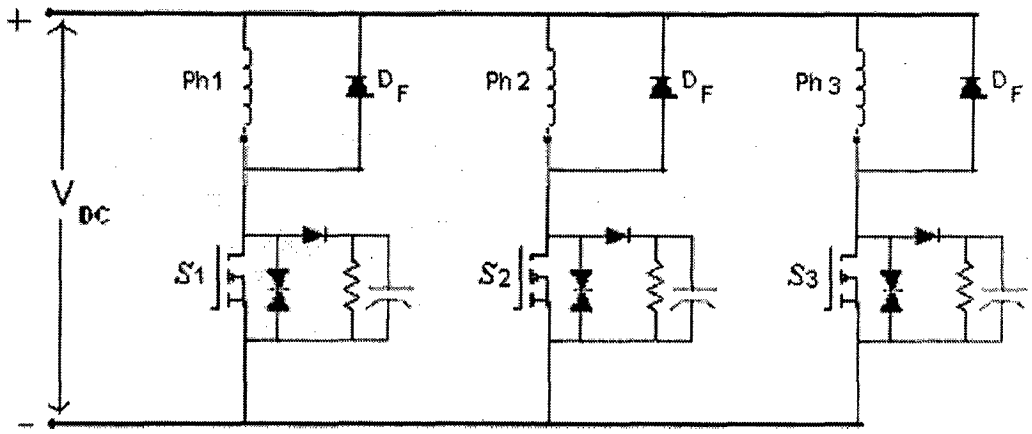

Fig 4.2 Power Circuit for 3-phase SRM

Pulse Amplification and isolation Circuit:

This circuit is used to provide isolation between power circuit and control circuit and also to amplify the pulse signal. This is shown in the figure 4.5.MCT2E → Optocoupler provides isolation between power circuit and control circuit.

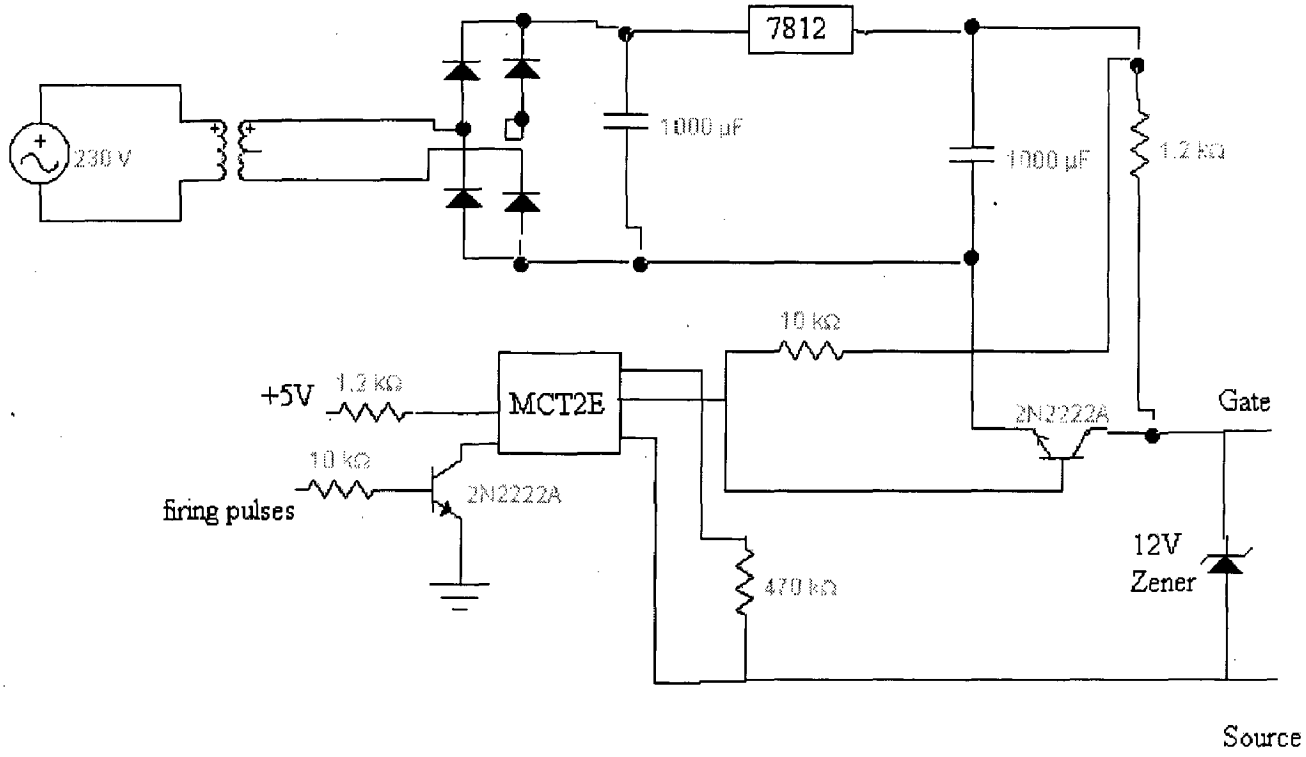

Fig 4.3 Gate driver circuit

Power supplies:

DC regulated power supplies (+12V, -12V, +5V) are required for providing the biasing to various transistors, IC's etc. The circuit diagram for various dc regulated power supplies are shown in figures 4.4a and b. In it, the single phase ac voltage is stepped down and then rectified using diode bridge rectifier. A capacitor of 1000micro farad, 50 V is connected at the output of the bridge rectifier for smoothening out the ripples in the rectified dc voltage of each supply. Voltage regulators chips 7812, 7912, and 7805 are used for obtaining the DC regulated voltages, +12V, -12Vand+5V respectively. A capacitor of 1000µf, 50V is connected at the output of the IC voltage regulator of each supply for obtaining the constant and ripple free DC voltage.

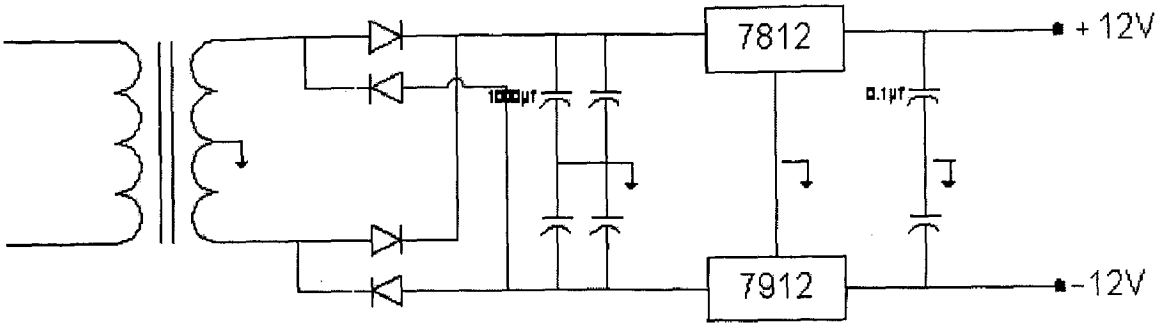

Fig 4.4 a +12V, -12V power supply

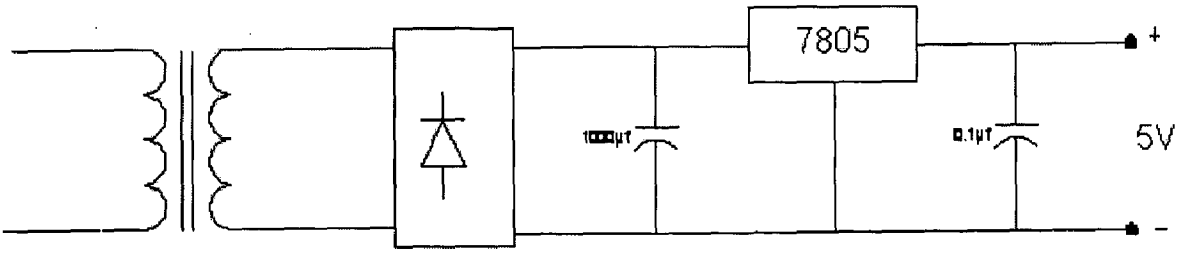

Fig 4.4 b +5V power supply

Protection of Mosfets

An RC snubber circuit is used for the protection of the main switching device. The circuit diagram is given in Fig. 4.5.

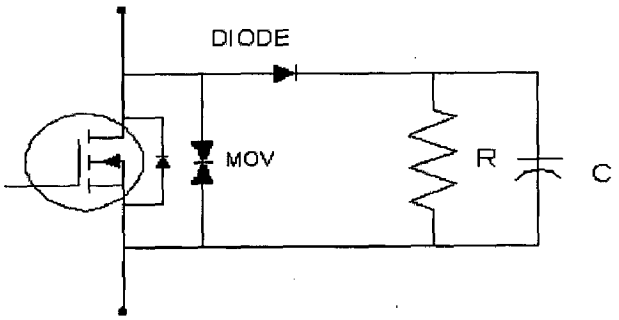

Fig.4.5 SNUBBER CIRCUIT FOR MOSFET PROTECTION

Energy stored in C, Ec=(1/2)*C*Vdc2

Power=Ec*fmax

This is the power dissipated PR in the resistor R.

Where VDC is the maximum DC level and fmax is the maximum frequency of the output wave.

This energy needs to be dissipated within Ton for the worst case i.e. Ton(min).

The time constant of the RC circuit is taken as one-fifth of Ton(min).

Therefore, TRC= 1/(5*6*fmax)=R*C

Constant losses in R for worst case are given by

P=VR2/R

Taking an average value of VR as 200V,P=8W

Also PR for VDC=400V and fmax=100Hz is 0.8W.

The value of R is found from the above equation for C=0.1μF and R comes out as 5 KΩ.

Current sensing circuit:

This circuit is used to sense the phase currents which can be used for the current control schemes such as Closed loop current control, hysteresis control etc. In the implementation the currents obtained are used for hysteresis control implemented in the microcontroller and also for closed loop operation. Figure 4.6 shows the current sensor circuit.

Closed loop Hall Effect current transducer is used to sense the current. The transducer use the ampere turn compensation method to enable the measurement of current from DC to high frequency with an ability to follow rapidly changing level or wave shapes. The application of primary current (Ip) causes a change in flux in the air gap. This in turn produces a change in output from hall element away from the steady state condition. This output is amplified to produce a current (Is), which is passed through a secondary winding causing a magnetizing force to oppose that of the primary current, thereby reducing the air gap flux. The secondary current is increased until the flux is reduced to zero. At this point the hall element output will return increased until the flux is reduced to zero. At this point the hall element output will return to steady state condition and the ampere turn product of secondary circuit will match that of primary.

The current that passes through the secondary winding is the output current. The transformation ratio is calculated by the standard current transformation equation

$$N_p I_p = N_s I_s$$

where

Np= primary current

Ns= secondary current

Ip= primary current

Is = secondary current.

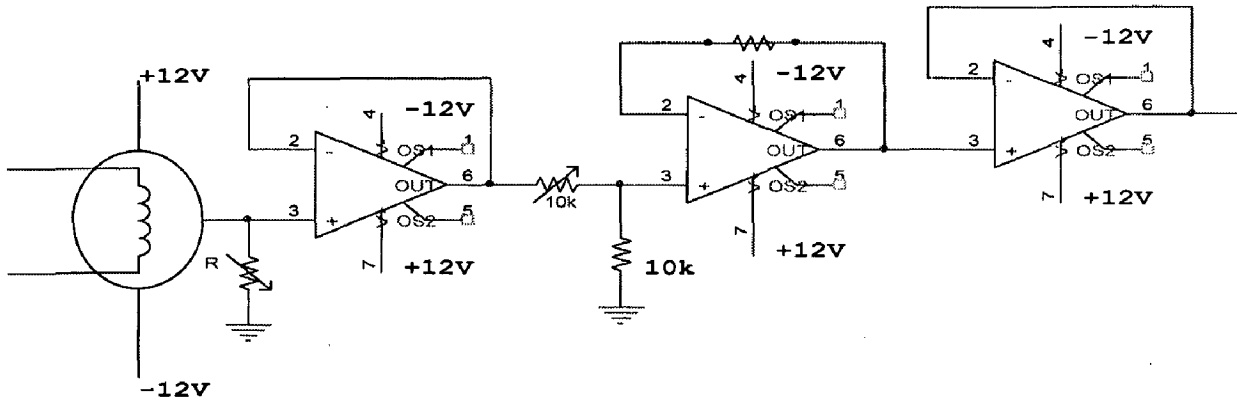

Fig 4.6 Current sensor circuit

Microcontroller Hardware Kit:

8751/8031 based Single Chip Microcontroller Kit manufactured by ANSHUMAN is used for the generation of signals.

Speed Encoder:

In order to get the optimum performance, the rotor position must be properly synchronized with the control pulses. The HEIDENHAIN ROD 436 Speed Encoder is used for position sensing to synchronize. It is designed to measure an angular displacement or a rotational speed.

The encoder has photo sensors and an LED which are arranged as shown in the figure 4.7. The photo sensors of the encoder are activated by the light of an internal LED. When the light is hidden, the sensor sends a logical "0". When the light passes through one of the slots of the encoder, a logical "1" is sent.

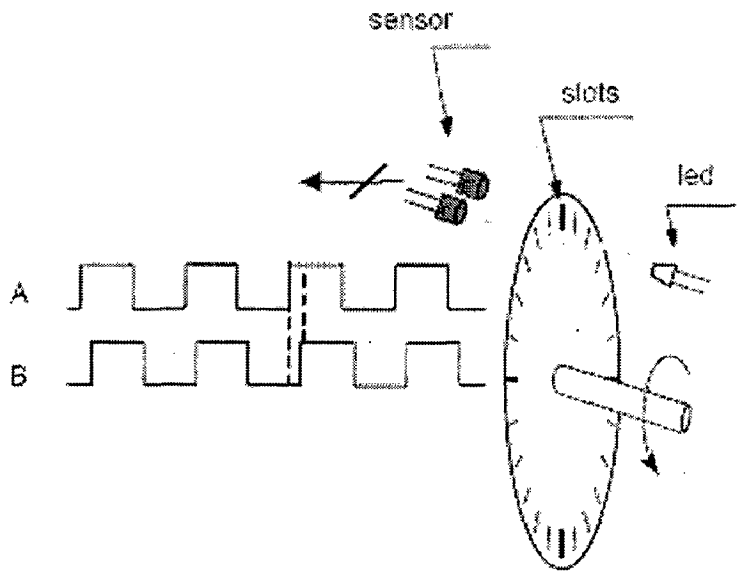

Fig.4.7 Speed Encoder

The encoder output has a socket with 12-pins. The pin structure and the socket layout are shown below:

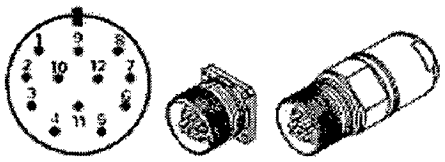

Fig. 4.8 Pin Socket of the ROD 436 Speed Encoder

Pin Number	Signal
1	$\overline{U_{a2}}$
2	10....30 V Sensor
3	U_{a0}
4	$\overline{U_{a0}}$
5	U_{a1}
6	$\overline{U_{a1}}$
7	$\overline{U_{aS}}$
8	U_{a2}
9	NC
10	0 V U_N
11	0 V Sensor
12	10...30 V U_P

Table 4.1 Table showing the Pin Numbers and Signals.

A supply voltage between 10 to 30 V is to be given. Signals are obtained from the pins as shown in figure 4.9. An index signal is also obtained from the encoder from which the direction of rotation can also be detected.

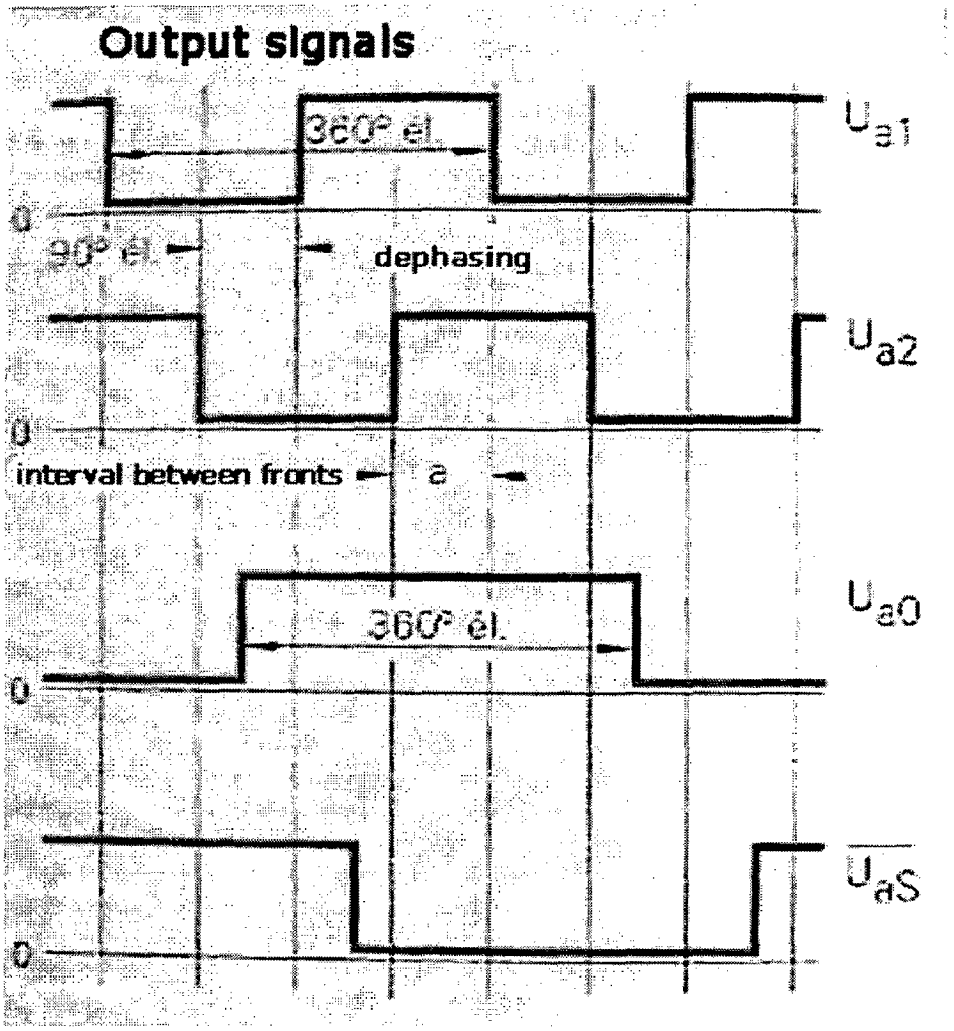

Fig. 4.9 Output signals from Speed Encoder ROD 436.

4.3 Interfacing and Circuit Connections

4.3.1 Speed Encoder Interfacing Circuit

The signals obtained from the pins of the encoder have a level which is almost equal to the supply voltage to the encoder. But, this level is not compatible to the signal to be given to the Timer of the Microcontroller which needs a TTL compatible signal. Also, the signals have a frequency range in Kilo Hertz which cannot be given to a simple transistor inverter circuit. So, a signal conditioning circuit is needed for these two purposes. The signal from the Encoder is given to a comparator circuit whose output is connected to a

2.2 KΩ pull-up resistor through a supply voltage of 5 V. The circuit diagram of the signal conditioning circuit is shown in figure 4.10.

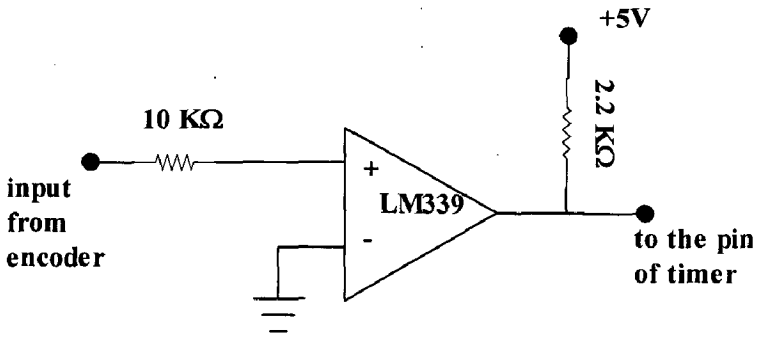

Fig. 4.10 showing the comparator circuit

4.3.2 Interfacing to the Timer and Power Circuit

The TTL signal from the signal conditioning circuit is given to the T1 pin of the Microcontroller. The Timer is programmed and the required control signals are generated from the 8255. As 8255 is already interfaced to the Microcontroller Kit, signals can be obtained from it. Pins PC3, PC4and PC5 are used to generate the control signals to the three MOSFETS. The signals from the 8255 are given to the pulse amplification and isolation circuits whose outputs are connected to the gates of the MOSFETS. The interfacing circuits are shown in figure 4.11.

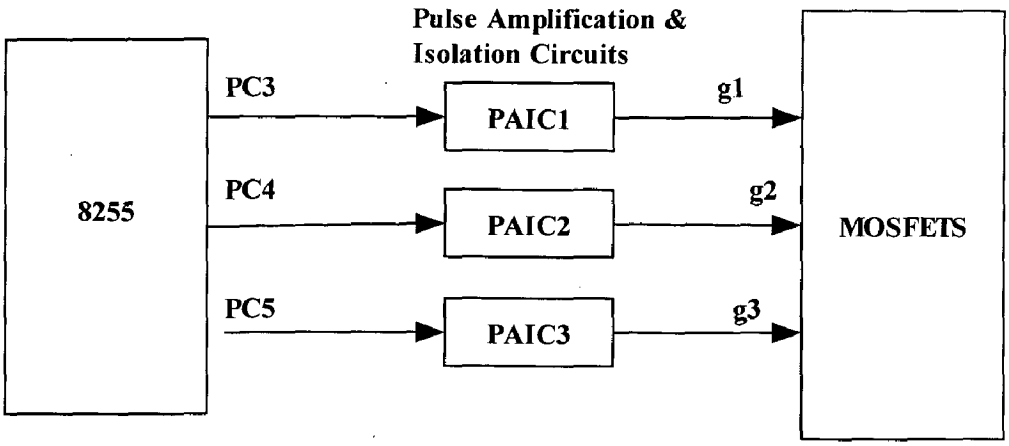

Fig. 4.11 showing the interfacing of the control signal from 8255 to Mosfets

4.4 Starting Problem

Starting problem of the SRM is to be considered in order to get the desired performance. Although a 6/4 pole SRM is designed so that it can start at any initial position, it cannot

rotate smoothly if the start problem is not correctly solved. The reason is quite clear from its operating principle. The phase-to-phase switching in the SRM drive must be precisely timed with rotor position to obtain smooth rotation and optimal torque output. Therefore, when starting the motor, the initial rotor position has to be exactly identified. That is, we have to know exactly where the rotor poles are aligned with respect to the exciting phase. Otherwise, proper commutation can't be guaranteed. Consequently, wrong commutation will lead to counter-desired torque blocking desired motion, which can even stop the rotation of the rotor.

In the project, a general starting scheme is used. The key idea of this method is to align one pair of rotor poles to one phase by a certain exciting current. And then use this position as reference position for the commutation. By doing so, the desired starting performance can be achieved.

During starting, one phase is excited with constant current for some period, for example, say Phase B. The rotor will align to Phase B along the shortest path under this exciting only if the generated torque is large enough to overcome the rotation friction. This exciting stator current should be able to align the rotor to the nearest exciting phase. While, the conduction period should be long enough to guarantee the finish of this aligning action. If the exciting period is too short, the rotor can't reach the aligned position due to load and friction; On the other hand, if the exciting period is too long, it will waste energy.

A value two thirds of the rated current of the SRM is chosen as the initial exciting current. If this current is large enough, the rotor will be able to move to the nearest aligned position. The rotor will rotate once there is one phase excited unless the rotor is already at the aligned position with respect to that phase. Also, it will hold the rotor at the aligned position if no other phases excited sequentially. When the rotor keeps stationary after the exciting, there are two cases for phenomenon: the exciting current is not large enough to generate rotation; the rotor itself is at the aligned position already. Obviously, we have to differentiate them for proper starting.

Hence, an additional method is needed. After exciting one Phase (say phase B), if the rotor remained stationary, then the exciting current is moved to its adjacent phase (Phase A or C) for the same period. If the rotor still keeps unmoved, it means that the

exciting current is too small to align the rotor and need to be increased. Otherwise, it means the rotor is already at the aligned position with the previous exciting phase (Phase B). In this case, the current aligned position can be taken as an initial reference position for commutation. In the cases where the load is unknown, this tuning procedure can be repeated.

In the project, following steps were followed for starting a 6/4 SRM:

Step1: Choosing the exciting current value.

Step2: Exciting phase B with the constant current. If the rotor remained stationary, go to step 3; otherwise, keep the exciting of this phase until the rotor stops;

Step3: Excite phase A with the same constant current. If the rotor keep stationary, increase the exciting current and go back to step2; Otherwise go to step4 when the rotor stops rotation;

Step4: The current aligned position is taken as the initial reference position. That is, the initial relationship between the stator and the rotor is that the rotor is at the aligned position with respect to phase A. And begin the control algorithm.

Then, the control algorithm is made to run after the above Start up Routine.

The flow chart for the Start-up Algorithm is shown in figure 4.12.

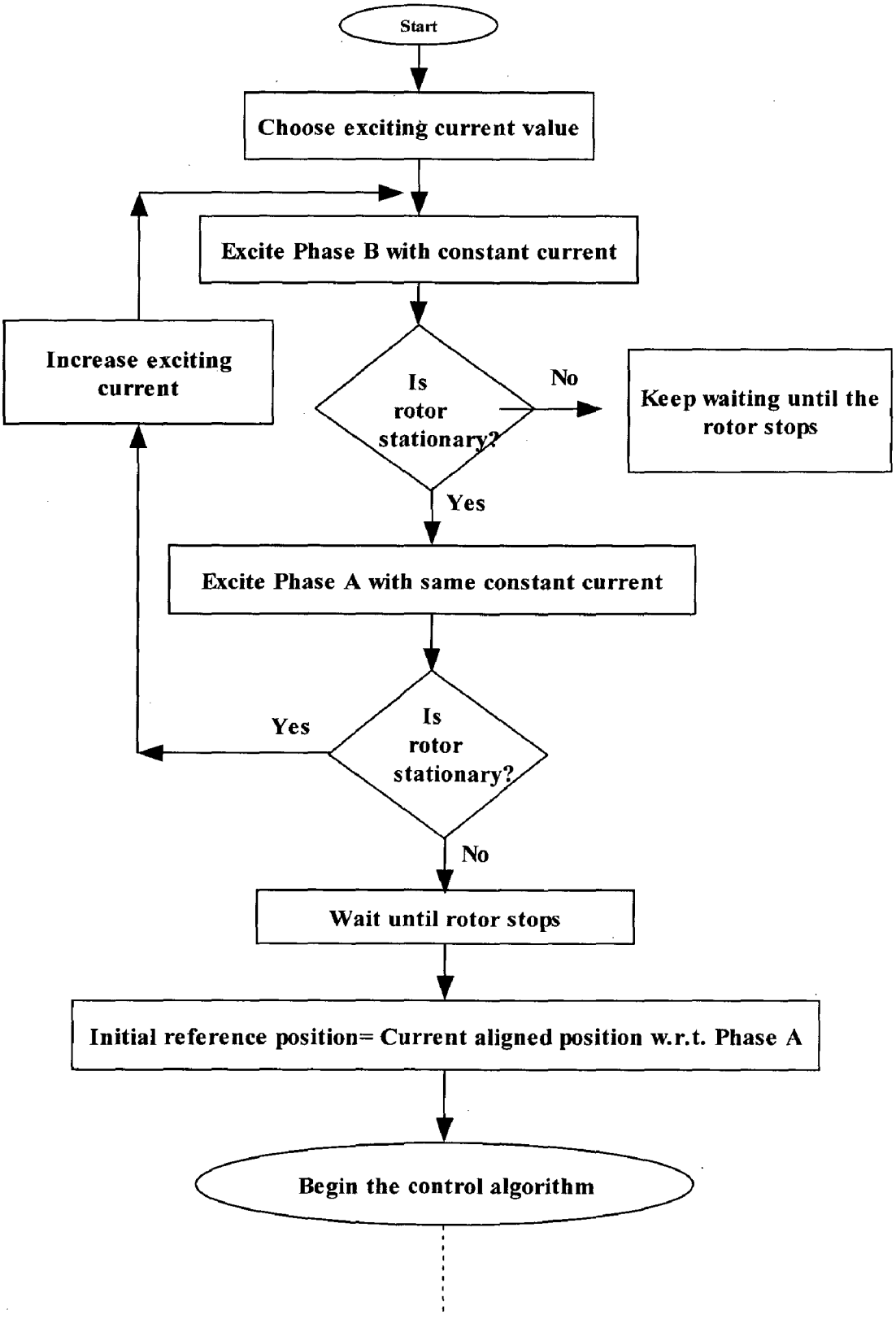

Fig. 4.12 Flow chart for the start up algorithm

4.5 Software Implementation

Microcontroller can be used for many applications in the implementation of an SRM Drive; some of them are given below:

Stroke Angle:

For a 6/4 SR motor, from an aligned position, the rotor will move 30 mechanical degrees before getting aligned with the next phase. For example, if the rotor is initially aligned when Phase A is excited and Phase B is to be excited. After energizing Phase B, the rotor will rotate 30 mechanical degrees before getting aligned with Phase B. This particular angle is called **Stroke Angle** (ε). In general, it can be calculated as

Stroke Angle, $\varepsilon = 360/ (m^* Nr)$ mechanical degree.

where m is the number of phases, Nr is the number of rotor poles.

Commutation Instants:

Rotor position information is used to generate correct commutation instants. The three Phases are to be energized with a phase shift equal to the Stroke Angle (here 30^o). The train of pulse from the Speed Encoder is used to obtain this phase shift.

Let m: No of pulses/rev (Fixed for Encoder) i.e., m pulses are obtained for 360 Degrees rotation.

No. of pulses for θ degree rotation= $(\theta^* m)/360$

For the Encoder used, m=5000;

For a 6/4 SRM, the number of pulses generated during a rotation of one Stroke angle, q = 416

This pulse count is used to generate the commutation instants. The Timer is programmed in such a way that it resets for every Stroke Angle. After every reset, the microcontroller is made to fire the pulses to the Phases sequentially depending upon the control algorithm.

Hysteresis Control:

Hysteresis control can be implemented with a microcontroller with very less complexity. The sensed phase currents are compared with the reference currents such that if $I_{sense} > I_{ref}$, the active phase is made to turn off until $I_{sense} <= I_{ref}$. This process is repeated for every few cycles of interval.

4.6 Open Loop Operation of a Microcontroller Based SRM:

Figure 4.13 show the experimental setup for the Microcontroller based SRM.

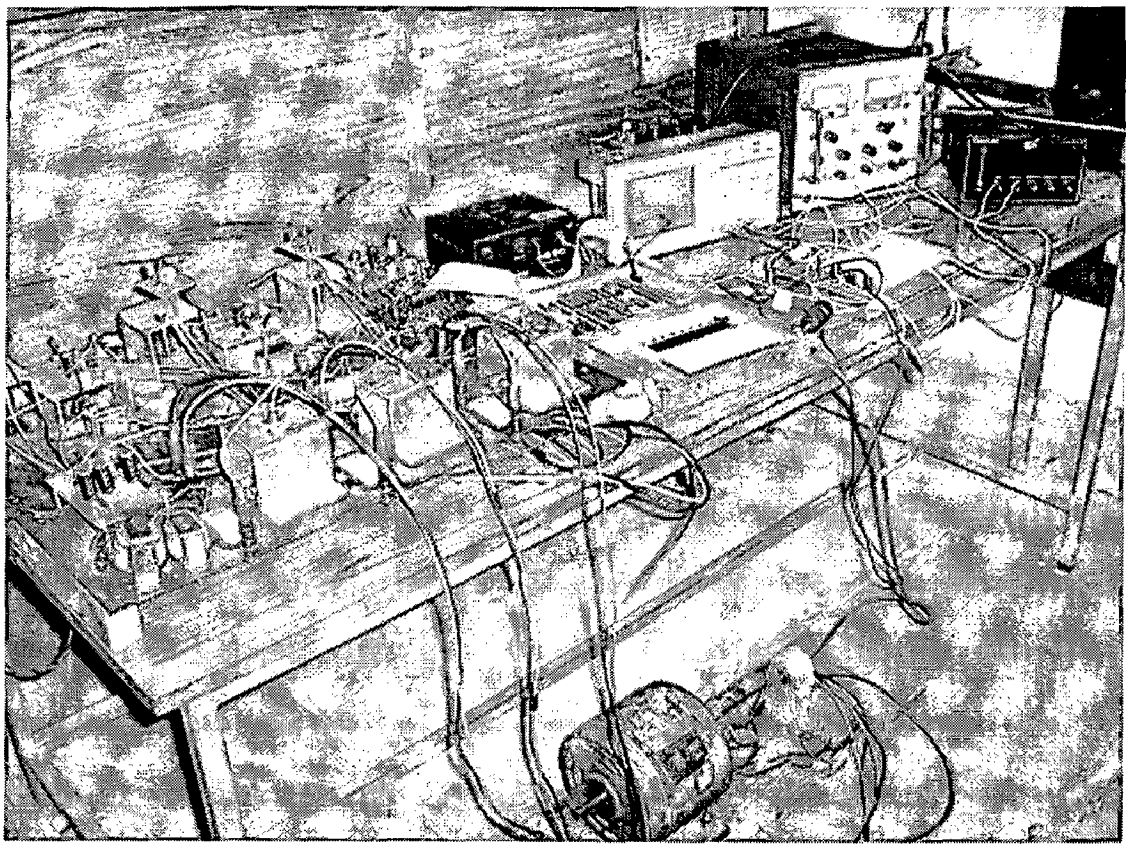

Fig 4.13 Experimental setup

The rotor position is obtained from the speed encoder which is connected to the T0/ T1 pin of microcontroller. The start up routine must be executed initially. The counter is loaded with an initial value such that it resets for every commutation threshold resulting with a set of TFX bit. After each reset of the counter the control is made to flow such that the next phase is excited (the output port pin corresponding to it is made to set). This is repeated to all the phases. A flowchart showing the implementation of open-loop operation of a microcontroller based SRM is shown in Fig 4.14.

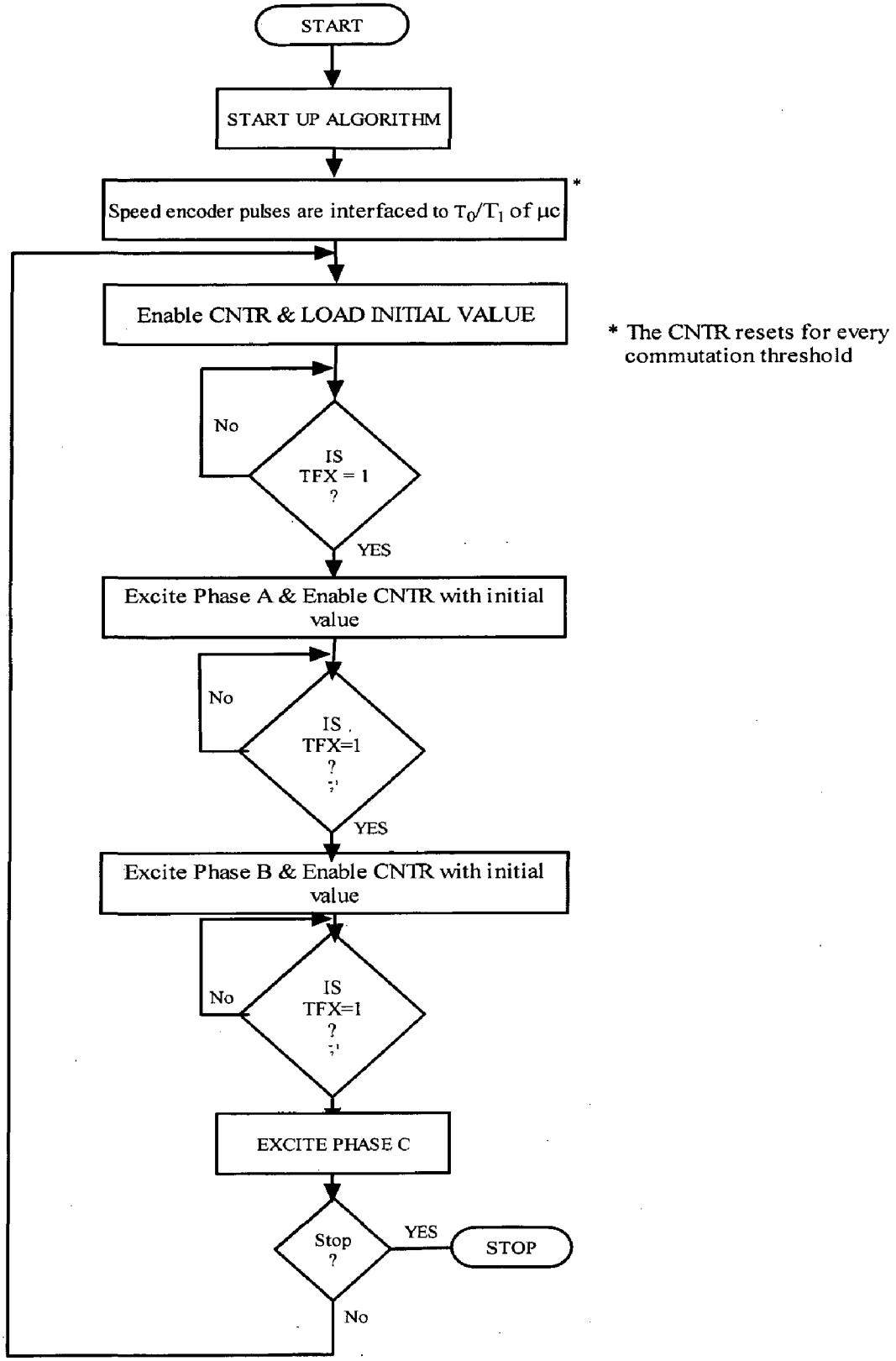

Fig. 4.14 Flow chart to show the open loop operation of SRM

4.7 Implementation of current controlled SRM

The control scheme is to be implemented with the microcontroller. The control algorithm is to be synchronized with the microcontroller timer. The phase currents are sensed and are compared with a reference. The comparator circuit chops the signal and gives the pulses when the phase current is less than the reference. The basic operation is same as that for an open loop operation. Fig 4.16 shows the flow chart to implement a current controlled SRM algorithm.

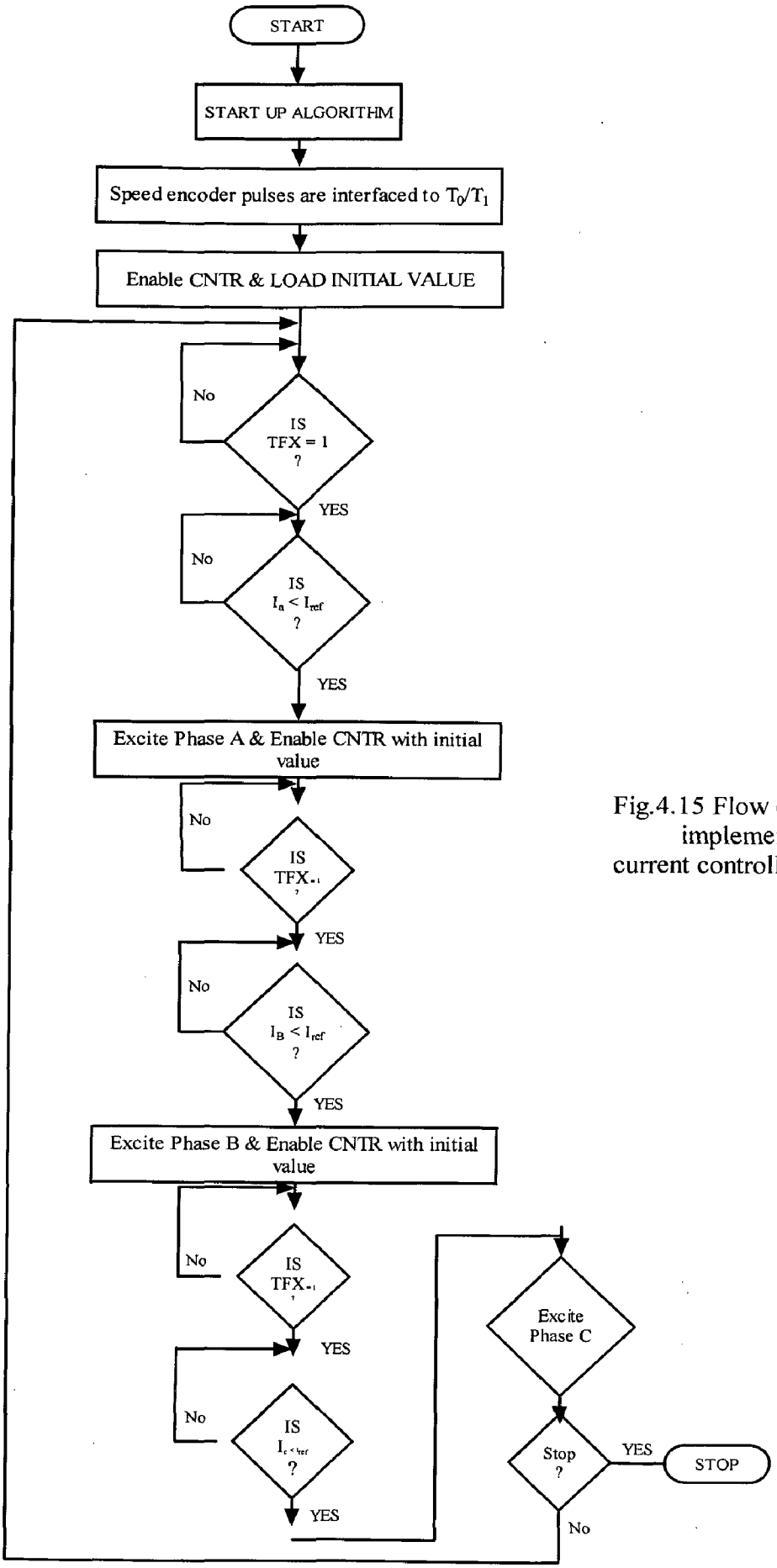

Fig.4.15 Flow chart to implement current controlled SRM

4.7 Conclusion

The hardware implementation for microcontroller based SRM drive is given. Various hardware circuits such as the power inverter circuit, pulse amplification and isolation circuit, power supplies, protection circuits, current sensing circuit etc are presented. Interfacing circuits for the implementation are given. The starting problem of an SRM is given with a solution algorithm. Flowcharts for the start up, open loop operation and current controlled SRM are presented.

Extensive simulations and performance investigations are carried out on the SRM drive. The simulation results of the drive for current control and speed control are presented in this chapter. The affect of step change in load and in the reference is studied. Simulations were done with varying excitation angles to know their affect on the performance characteristics. The optimum excitation angles for the speed control are determined. Also, the maximum load that can be applied for a particular excitation angle is determined.

5.1 Current controlled SRM

The simulation results for the current controlled SRM shown in figure 3.6 are given below: The motor is made to run with turn on angle= 0^{o} and turn off angle= 38^{o}.The speed response for a reference current is 8 A is shown in figure 5.1. The steady state speed is 146.5 rad/sec with a settling time = 0.4 sec. The ratings of the Machine are given in Appendix I.

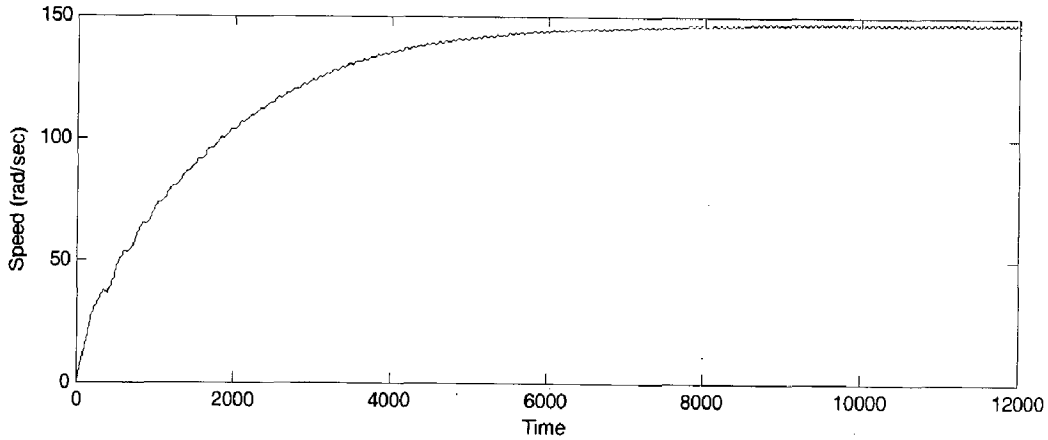

Fig. 5.1 Speed response for the Current Control of SRM with I_{ref}= 8 A

A response showing the voltage, inductance, current and torque of one phase is given in figure 5.2(a) and 5.2 (b). They show clearly the application of excitation during the positive slope of inductance to get a positive torque. In order have a better insight; the phase inductance is multiplied by 100 and voltage by 0.1.Figure 5.2 (b) shows how the phase voltage is chopped after reaching the reference current. Figure 5.3 shows the phase

torques and figure 5.4 shows the phase inductances of SRM. Figures5.5 and 5.6 shows the phase torque and current of SRM.

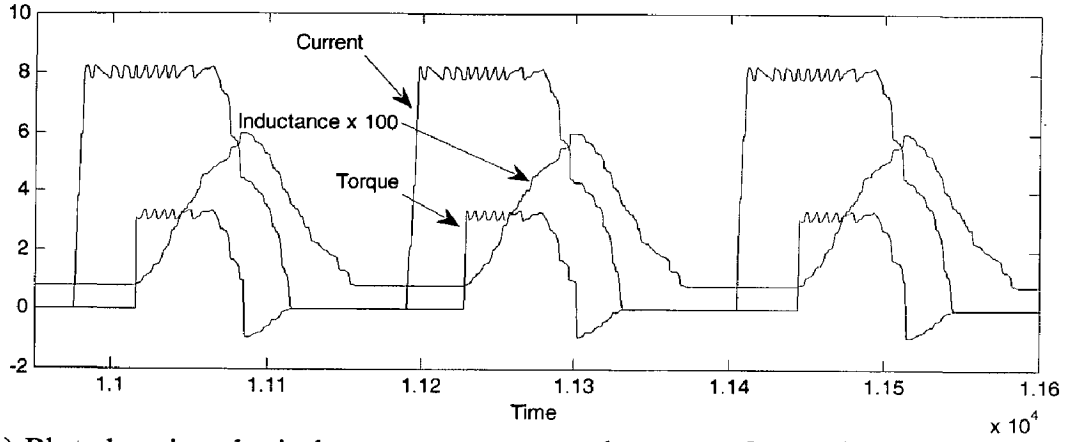

Fig. 5.2(a) Plot showing the inductance, current and torque of one phase of SRM

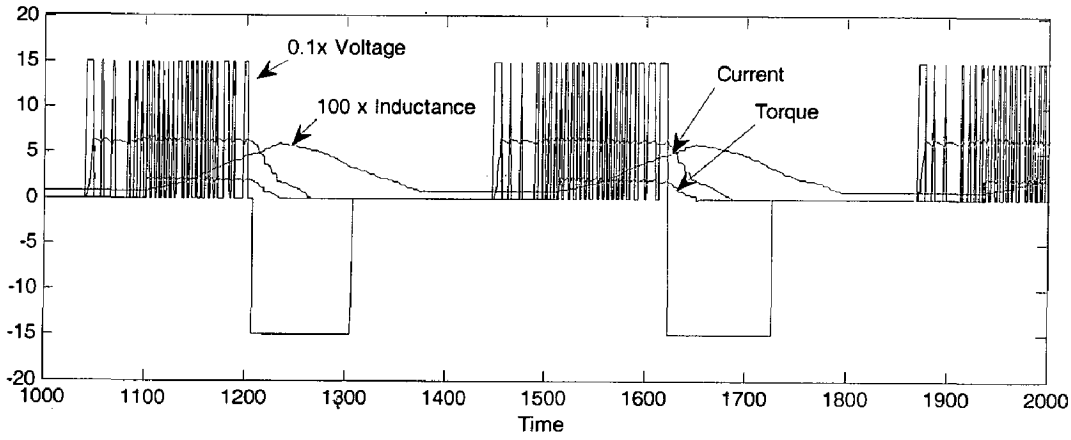

Fig 5.2 (b) Plot showing the voltage, inductance, current and torque of one phase of SRM

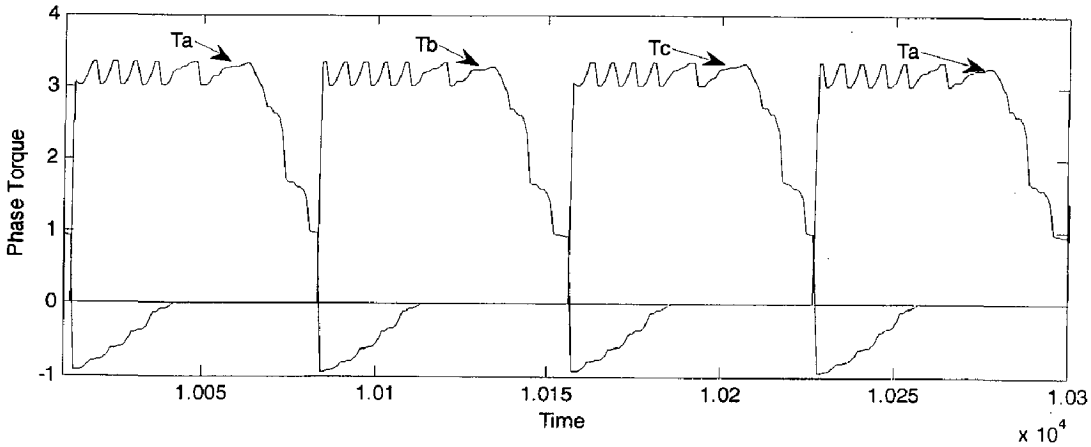

Fig 5.3 Plot showing the phase torques of the SRM

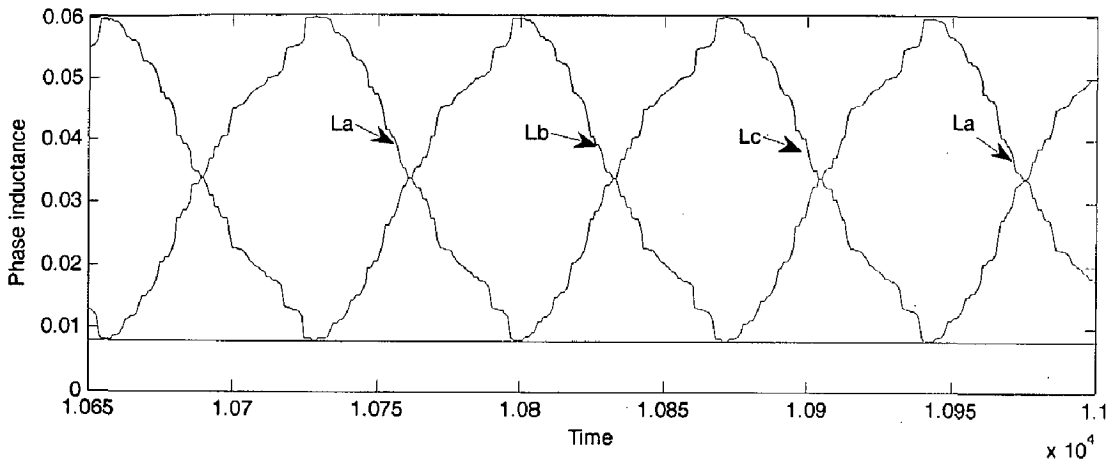

Fig 5.4 Plot showing the inductances of three phases of SRM

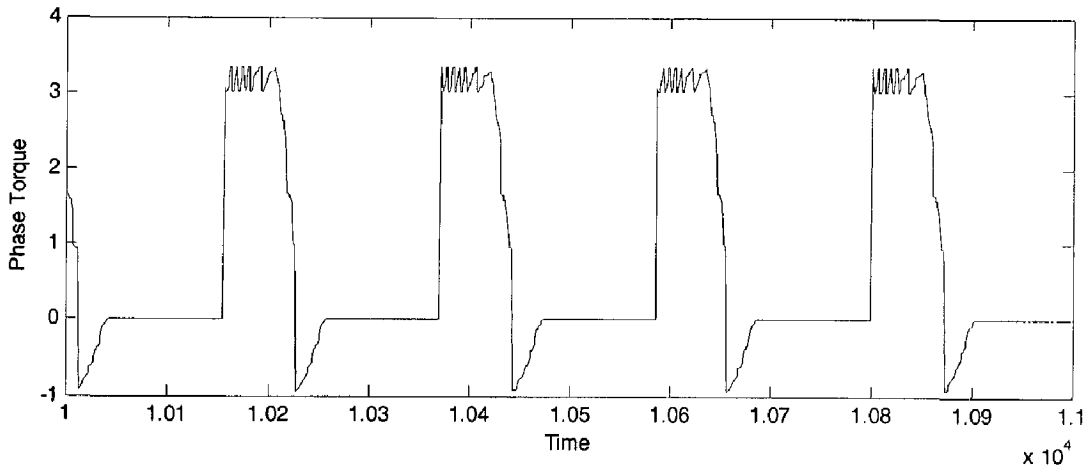

Fig. 5.5 Plot showing the phase torque of SRM

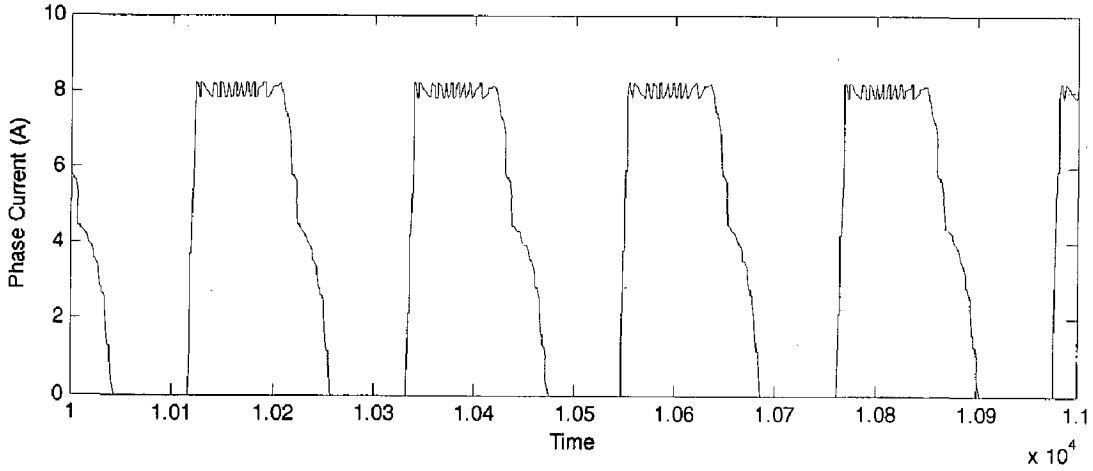

Fig. 5.6 Plot showing the phase current of SRM

5.1.1 Speed response for a step change in load:

Figure 5.7 shows the speed response of the current controlled SRM drive for a step change in load of 0.1 N-m. Initially, a step change from no load to 0.1 N-m is applied at t=0.6 second, and later it is removed at t=1.2 sec. The initial speed before application of load = 146.5 rps. The speed after the application of load has ripple which varies from 142 to 142.5 rps. The settling time of which is 0.1 sec. When load is removed, the speed increases to 146.5 rps with a settling time of 0.1 sec.

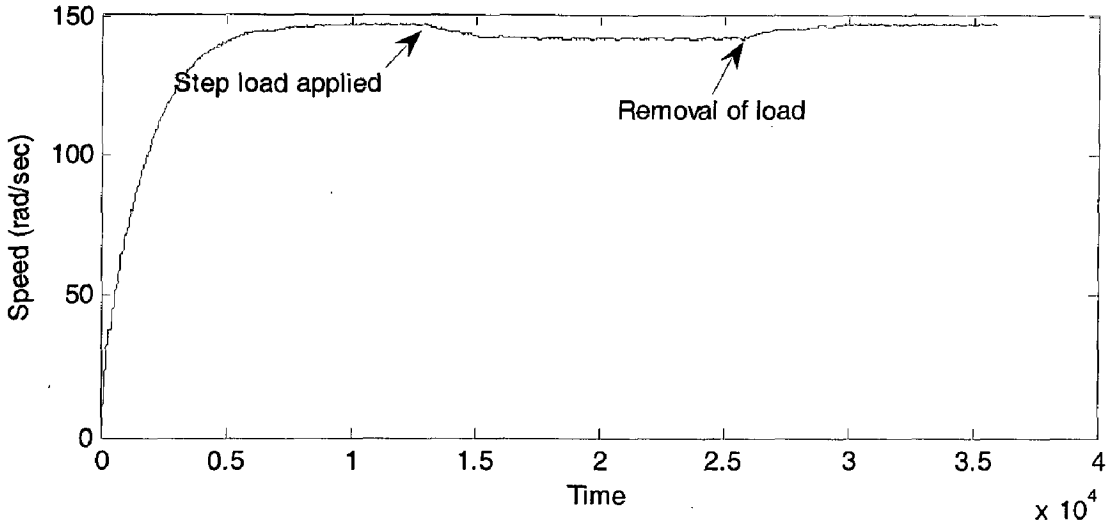

Fig. 5.7 Plot showing the speed response for a step change in load

5.1.2 Speed response for a step change in current reference

Figure 5.8 shows the speed response for a step change in current reference. Initially, the current reference is 8 A, it is changed to 10 A and then, back to 8 A. Initially, the steady state speed is 146.5 rps, upon a change in current reference to 10 A, the speed ripple is between 164.8 and 165.8. The settling time is 0.1 sec. Upon changing the current reference back to 8 A, the speed decreases back to 146.5 with a settling time of 0.35 sec. Figure 5.9 shows the plot of electromagnetic torque of the drive. The peak value of the torque before change in current reference is 3.34 N-m and the steady state torque peak value for current reference of 10 A is 3.65 N-m. A sudden rise of torque

appears which can be seen in the figure after the change in current reference, it happens to be 4.34 N-m. Figure 5.9 shows the plot of phase current.

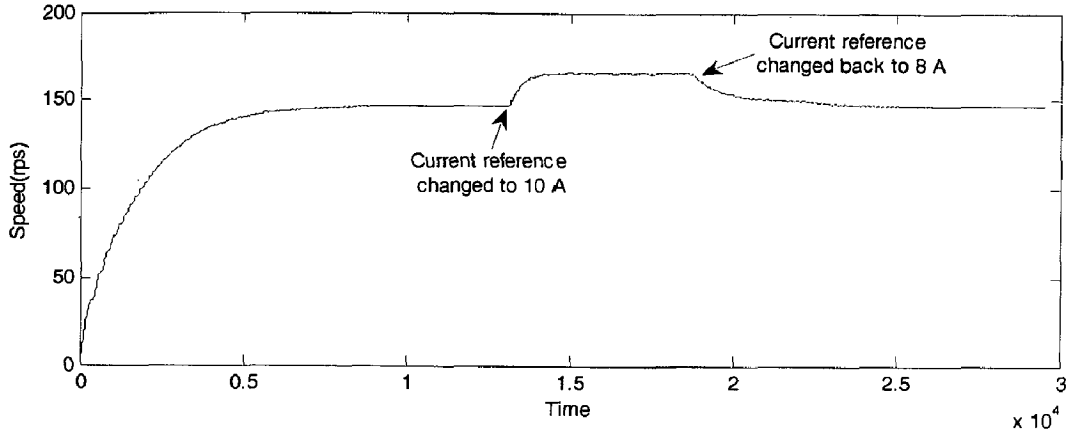

Fig. 5.8 Plot showing the speed response for a step change in current reference

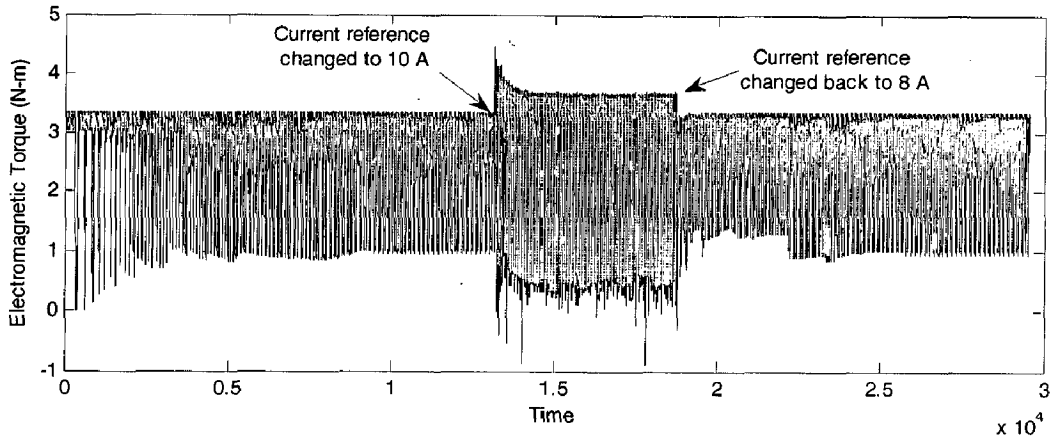

Fig. 5.8 Plot showing the Electromagnetic Torque for a step change in current reference

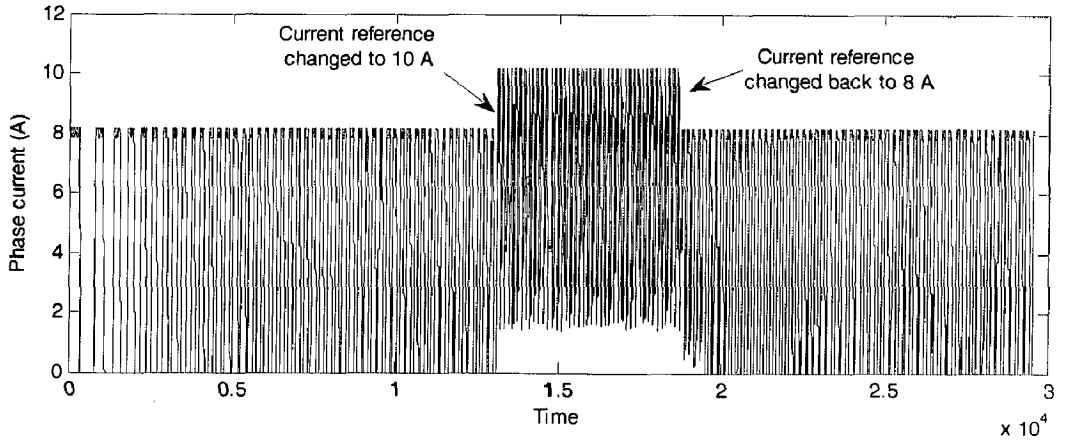

Fig. 5.9 Plot showing the phase current for a step change in current reference

5.2 Speed control of SRM

5.2.1 Speed response without using Simulink block

Figure 10 (a) shows the speed response of the SRM using Simulink block under no load. The speed reference is 210 rps. The settling time is 0.28 sec with a speed ripple between 209.8 to 210.2 rps. The machine details are given in Appendix II.

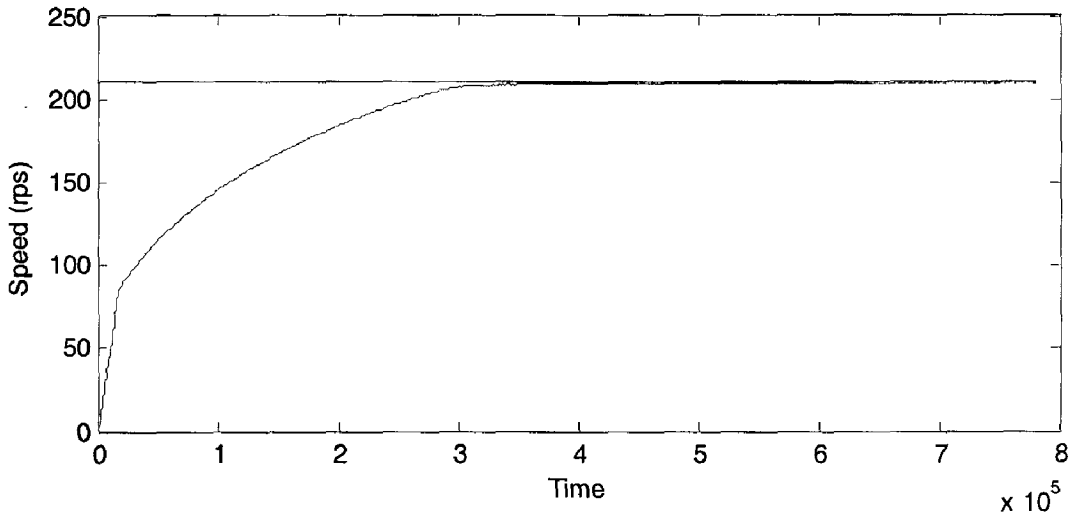

Fig. 5.10 (a) Plot showing the speed response of a speed controlled SRM

5.2.2 Speed response for a step change in load

Figure 5.10 shows the speed response for speed control of SRM for the figure 3.9. The reference speed is set to be at 100 rps. The settling time of response for no load is 0.05 sec with an overshoot to 106 rps. A step load of 5 N-m is applied at 0.6 sec. The speed dip is 11 rps with a settling time of 0.09 sec. The steady state peak to peak ripple is between 99 to 101 rps. After the removal of load at t=1.2 sec, the speed rises suddenly by 9rps with a settling time of 0.05 sec. At steady state, the speed ripple is between 99.6 to 100.4 rps. Fig. 5.11 shows the plot of electromagnetic torque. The peak value of the torque changes from 2.3 to 8.3 N-m upon the application of a load of 5 N-m. Fig 5.12 shows the plot of phase current, its peak value changes from 6.8 A to 13.5 A upon the application of load.

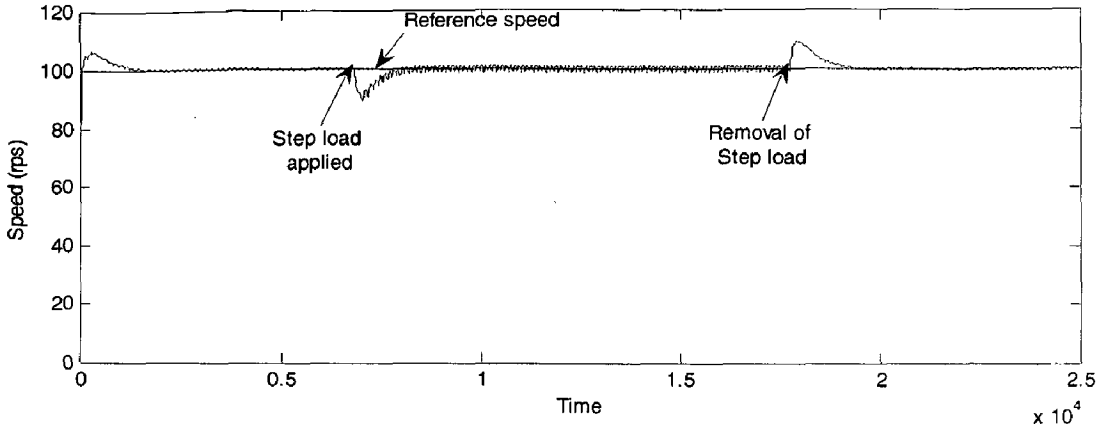

Fig. 5.10 Plot showing the speed response for a step change in load for speed control of SRM

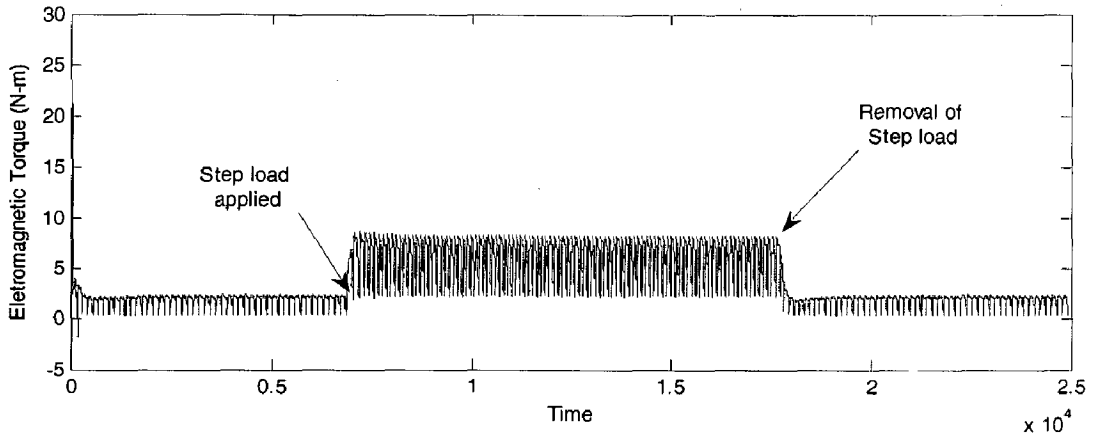

Fig. 5.11 Plot showing the electromagnetic torque for a step change in load

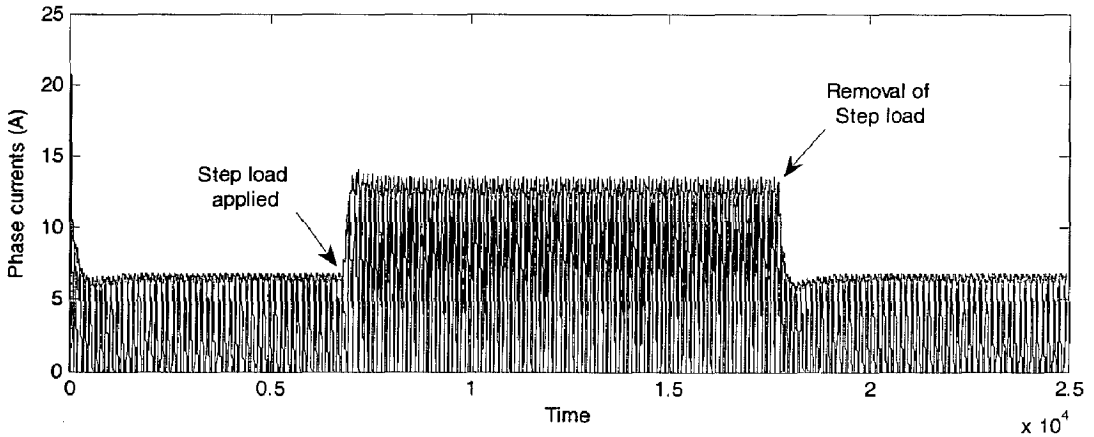

Fig. 5.12 Plot showing the phase current for a step change in load

5.2.3 Speed response for a step change in speed reference

Figure 5.13 show the plot of speed response for step change in speed reference. The reference speed change from 100 rps to 90 rps and back to 100 rps. The speed dip is around 2 rps with a steady state speed ripple between 89.5 to 90.3 rps. The settling time is 0.05 sec. When reference is changed back to 100 rps, the speed rise is 1 rps with a steady state speed ripple between 99.5 to 100.4 rps. The settling time is 0.05 sec. Fig 5.14 shows the electromagnetic torque of SRM. The torque dip is from 2.2 to 0.2 N-m when reference speed is decreased to 90 rps while the torque rise is from 2.2 to 5.2 N-m when speed is increased back to 100 rps. Fig 5.15 shows the plot of phase current.

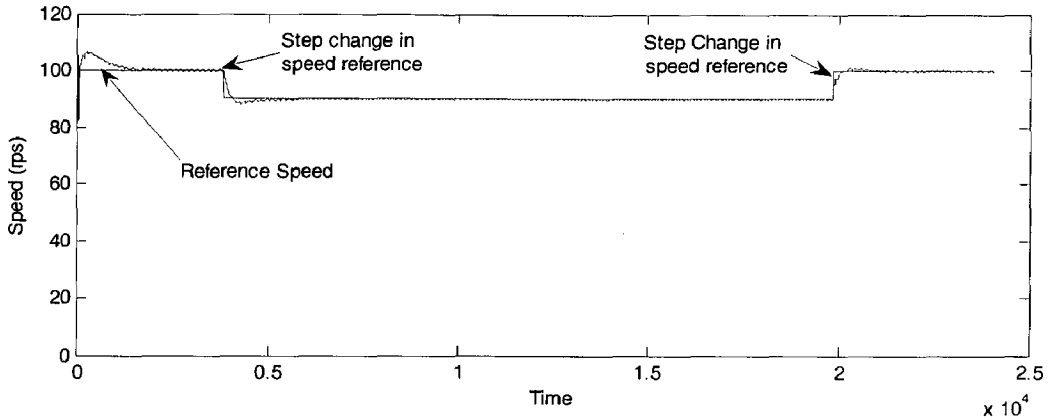

Fig. 5.13 Plot showing the speed response for a step change in speed reference

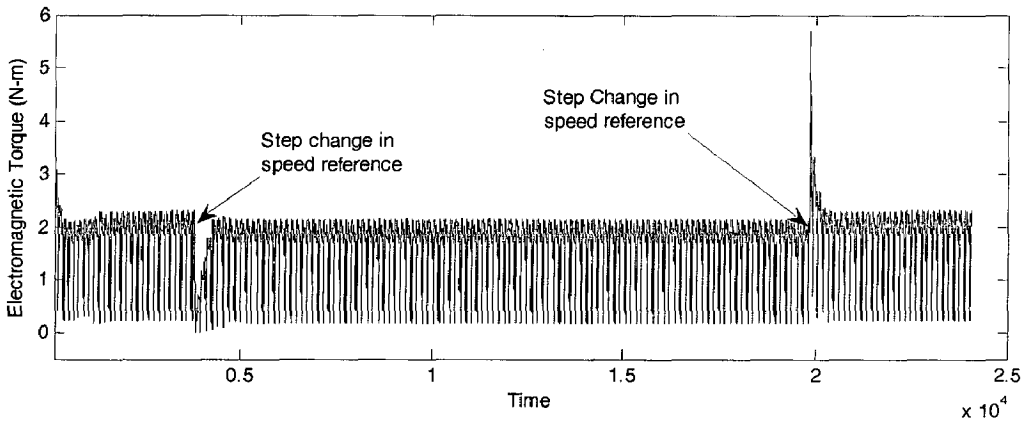

Fig. 5.14 Plot showing the electromagnetic torque for a step change in speed reference

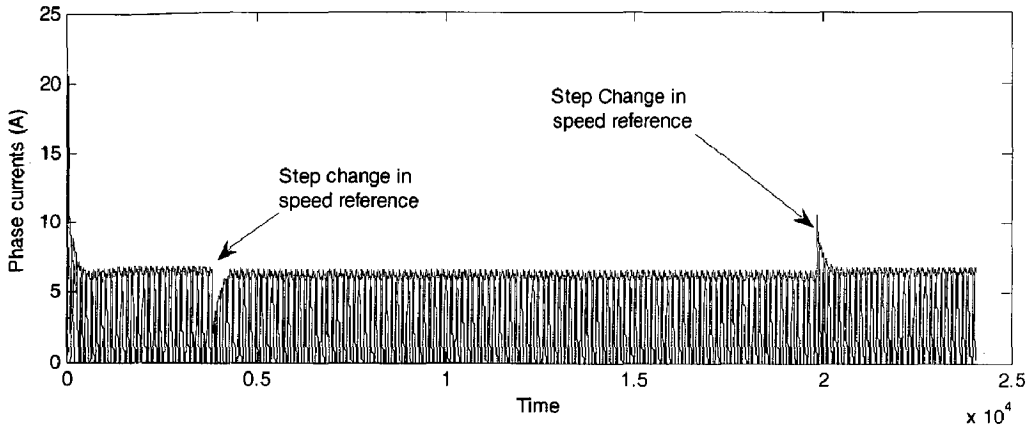

Fig. 5.15 Plot showing the phase current for a step change in speed reference

5.2.4 Speed response for fuzzy controlled SRM

Figure 5.16 shows the speed response for fuzzy controlled SRM. The reference speed is 100rps. The settling time is 0.029 sec and the steady state speed is 98 rps.

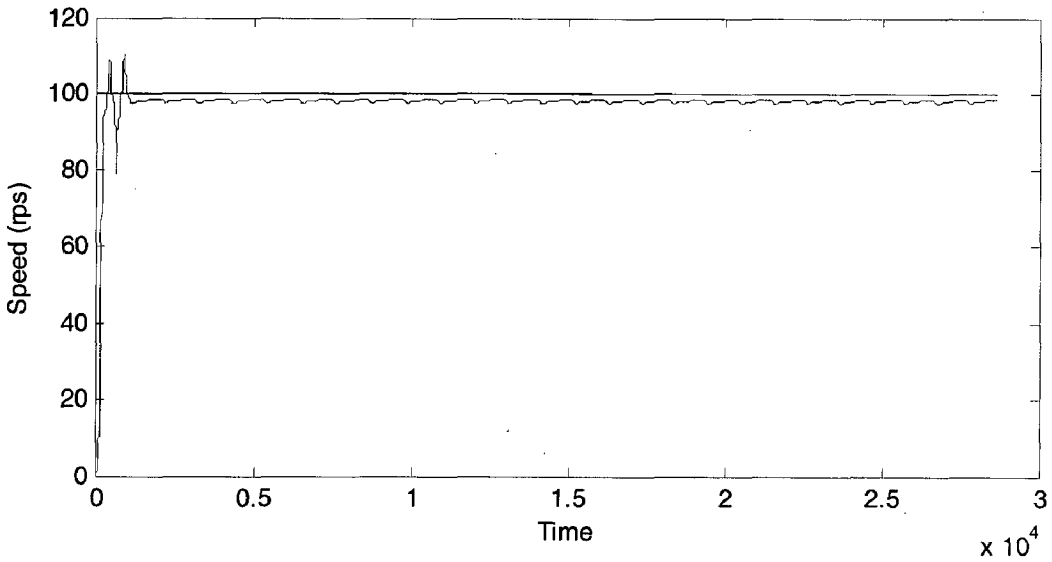

Fig. 5.16 showing the speed response for a Fuzzy Controlled SRM

5.3 Impact of switching angles on the Performance of SRM drive system

For forward motoring, the appropriate stator phase winding must remain excited only during the period when rate of change of phase inductance is positive. Else, the motor would develop braking torque or no torque at all. The stator phase must be excited when its inductance starts rising and must be de-excited when the phase inductance ceases to increase. The switching function thus must ensure that current in phase winding reaches

its reference value at the desired instant of inductance rise and is again brought to zero when inductance reaches its maximum and does not increase further. Due to delay in current rise and fall on account of winding inductance, the switch must be closed at a turn-on angle (also called advance angle) θ_{on} and must similarly be opened at a turn-off angle θ_{off}. These switching angles are variable and depend mainly on speed and desired current in phase windings of SRM. The significance of turn off and turn on angles is presented below:

5.3.1 Turn off angle

Turn-off angle plays an important role in developing electromagnetic torque in Switched Reluctance Motor (SRM) and leads to stable or unstable operation of the drive. The value of turn-off angle is usually variable and depends upon the motor speed and other parameters of the inverter that excites the SRM. A study is conducted for full-load and partial load starting and operation of the drive with fixed turn-off angle control scheme. The simulated performance of SRM drive system is presented to analyze the effect of fixed value of turn-off angle on transient and steady state performance of the drive in terms of speed response.

The present work analyzes the performance of SRM drive with different values of fixed turn-off angles and recommends an optimum value that gives an acceptable performance of the drive. The turn-on angle remains fixed during the study. The drive performance in terms of speed is presented. Simulated results pertaining to starting time, overshoot, steady state error, settling time and speed ripple are also presented. Since, PID controller offers a simple control structure to achieve an optimum performance; it is used for predicting the drive performance.

The study is conducted with a fixed turn on angle and the turn off angle is varied. In the study, a turn on angle $\theta_{on} = 0^{\circ}$ is used and the turn off angle θ_{off} angle is varied from 34 to 44 degrees in steps of 2 degrees with a load torque of 5 N-m. The speed response for different turn off angles is shown in figure 5.17. Figure 5.18 shows the steady state speed response. Turn off angle of 44° results in failure of start at full load. Table 5.1 shows the maximum and minimum speed ripple for different turn off angles.

Turn off angle (in degrees)	Maximum speed of ripple (in rps)	Minimum speed of ripple (in rps)	Peak to peak speed ripple (in rps)
34	102.5	96.5	6
36	102	98	4
38	101.5	99	2.5
40	102.2	97.7	4.5
42	110	72	38

Table 5.1 showing the speed ripple for various turn off angles

As the turn off angle increases, the settling time increases and the rise time decreases. The speed ripple is less for a turn off angle of 38°. 38° is an optimum value of turn-off angle which gives ideal performance in terms of defined indices as its speed rise is reasonably fast throughout and its steady state ripple is less.

Turn off angle above 43° results in failure of start at full load. However, a reduction in load torque to 1.5 N-m permits the use of higher turn off angles and the maximum value of turn off angle that ensures successful acceleration to rated speed. To determine the maximum load that can be allowed for a particular maximum turn off angle, first the load torque equal to half the rated, 2.5 N-m is applied. The speed response is observed for decreasing different loads, and the maximum load torque that can be applied for maximum turn off angle is determined and it turns out to be 1.5N-m. Fig. 5.19 shows the speed response for different loads with a turn off angle of 43°.

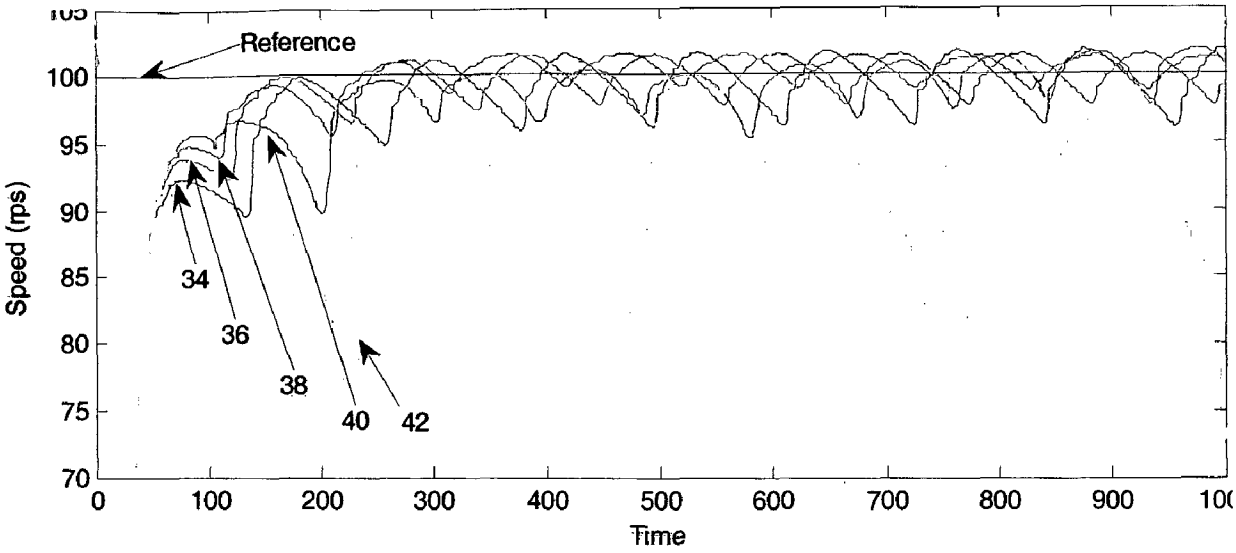

Fig. 5.17 Plot showing the speed response for different turn off angles

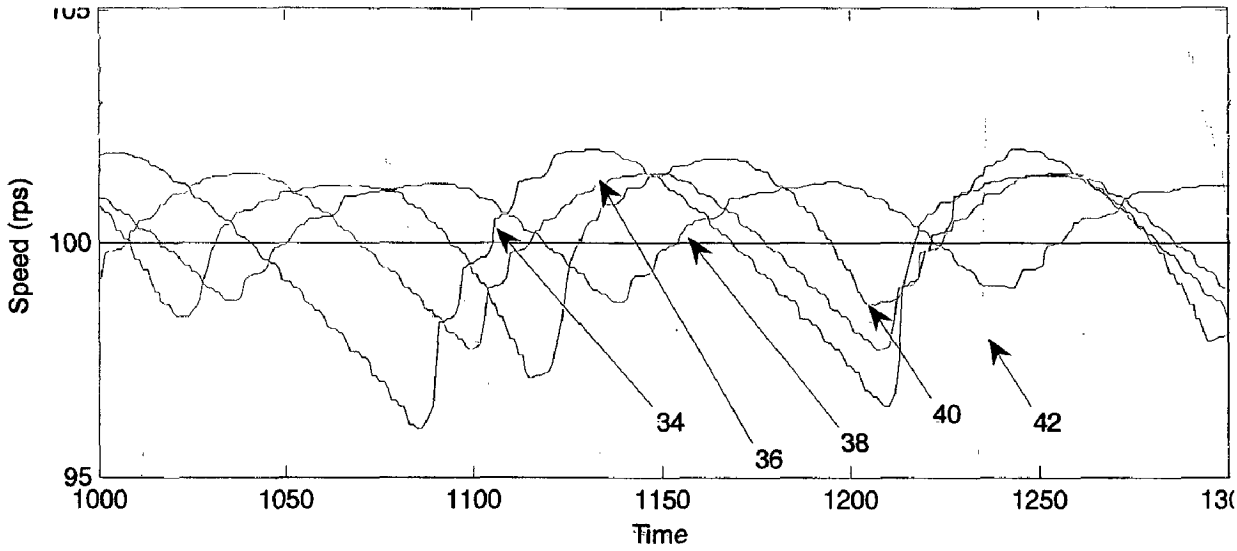

Fig. 5.18 Plot showing the steady state speed response for different turn off angles

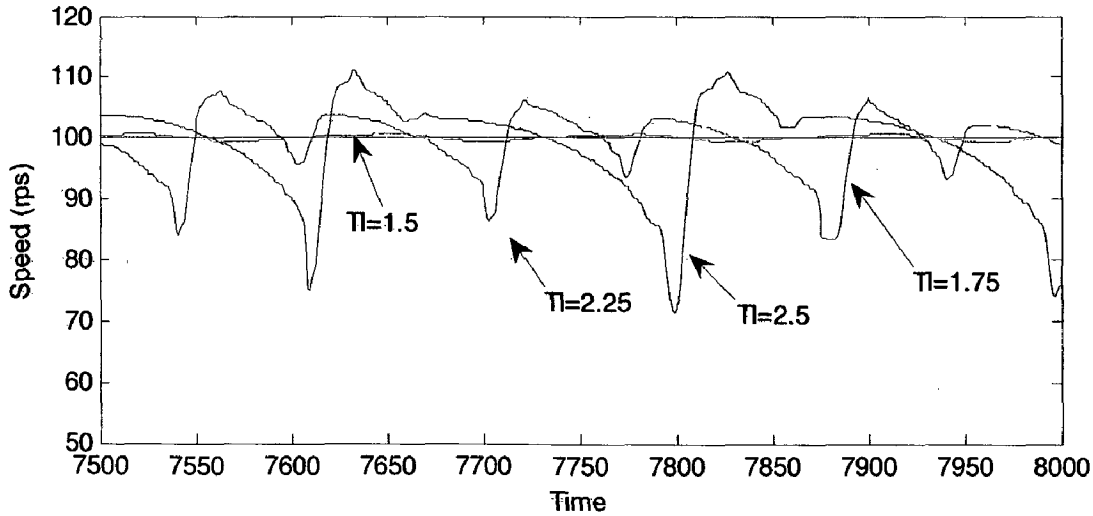

Fig. 5.19 Plot showing the speed response for different loads with turn off angle of 43°

5.3.3 Turn on angle

Due to the delay in current rise on account of winding inductance, the switch must be closed at a turn-on angle (also called advance angle) θ_{on}. Phase advancing is necessary to establish the phase current at the onset of rotor and stator pole overlap region. Fig 5.2(a) shows the phase inductance, current and torque with turn on angle = 0°. The inductance starts to increase from 15° onwards; hence in this case an advance angle of 15° is present. Due to this a maximum torque is obtained during the positive slope of the inductance. Figure 5.20 shows the speed response for different turn on angles from 0 to 15 °. It is seen that as the turn on angle increases (i.e., advance angle decreases), speed response becomes worse.

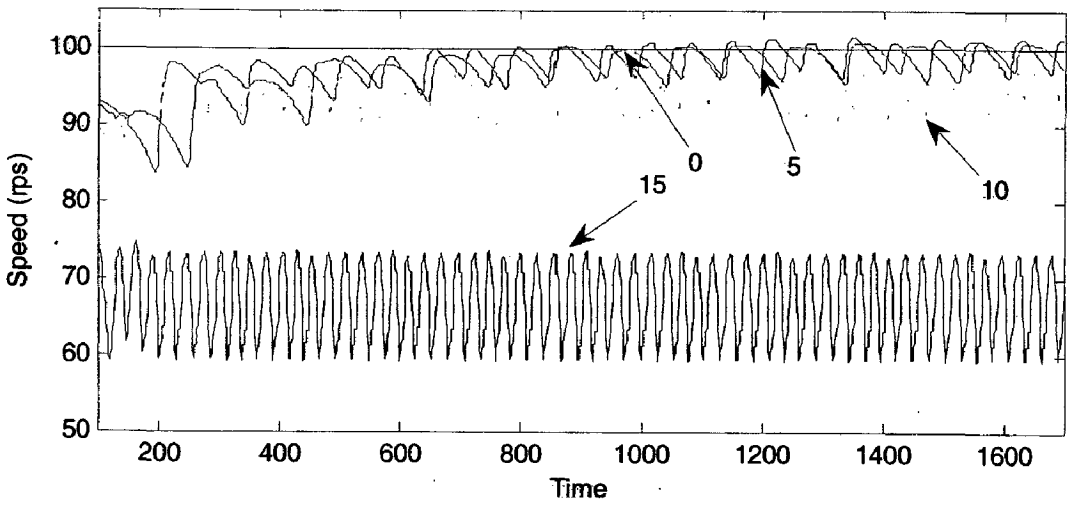

Fig. 5.20 Plot showing the speed response for different turn on angles

5.3 Experimental Results

The output signals from the speed encoder have a voltage level equal to its supply voltage. It is conditioned through a comparator to get a TTL signal. Fig 5.21 shows both the encoder and TTL signals. The microcontroller generates the control signals from the 8255. Figure 5.22 shows the gating signals from 8255. It is clear from the waveforms that at any instant only one phase is turned on. Figures 5.23 (a), (b), (c) show the voltage across drain and source (V_{DS}) when each signal obtained from 8255 are given to mosfets through pulse amplification and isolation circuit.

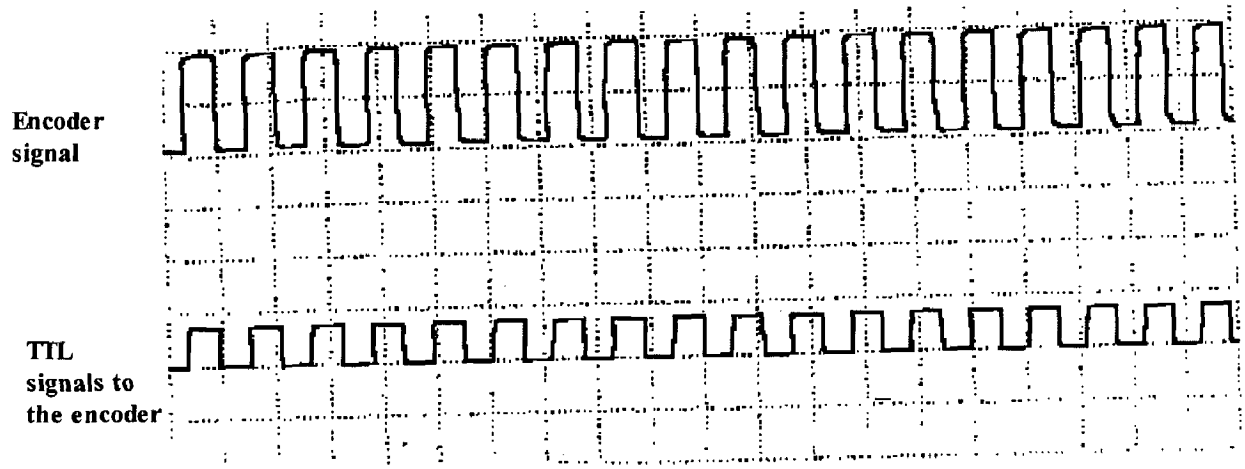

Fig. 5.21 Waveforms showing the speed encoder and comparator output signals

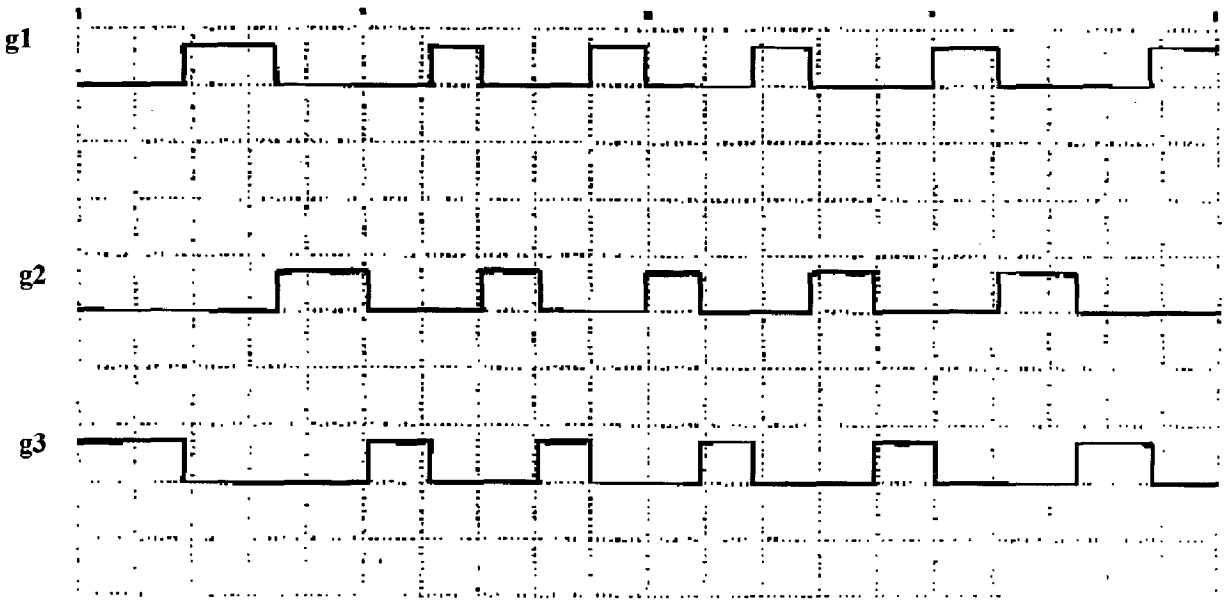

Fig. 5.22 Waveforms showing two gating signals from 8255

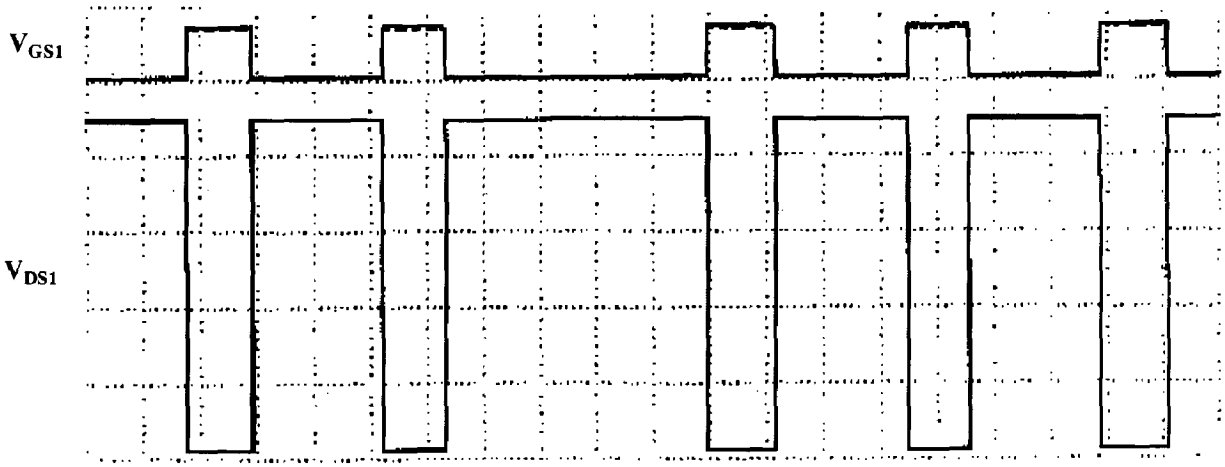

Fig 5.23 (a)

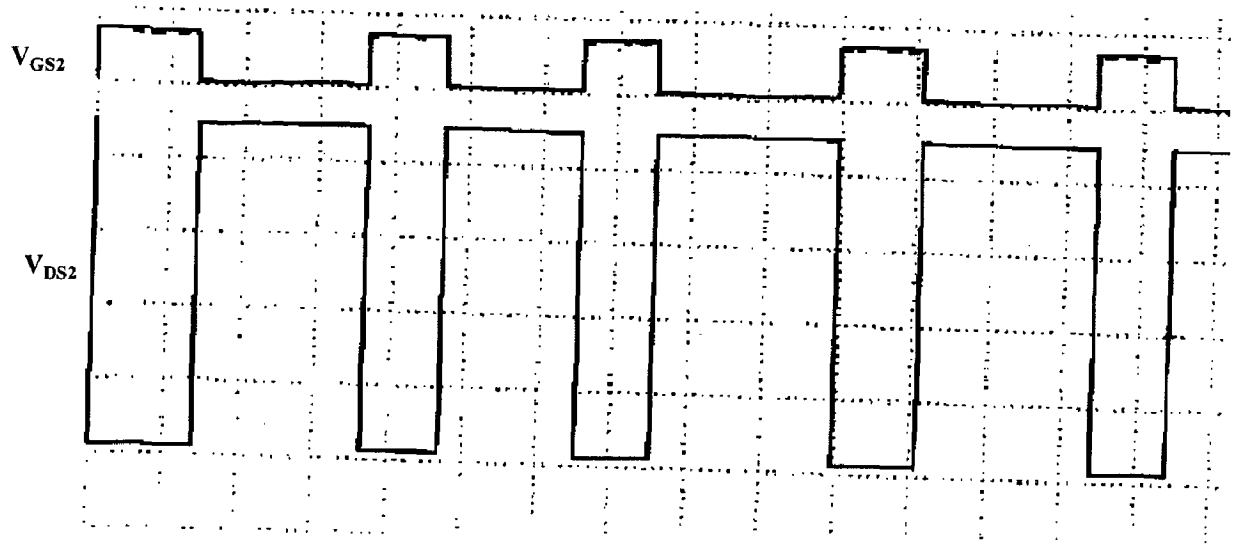

Fig 5.23 (b)

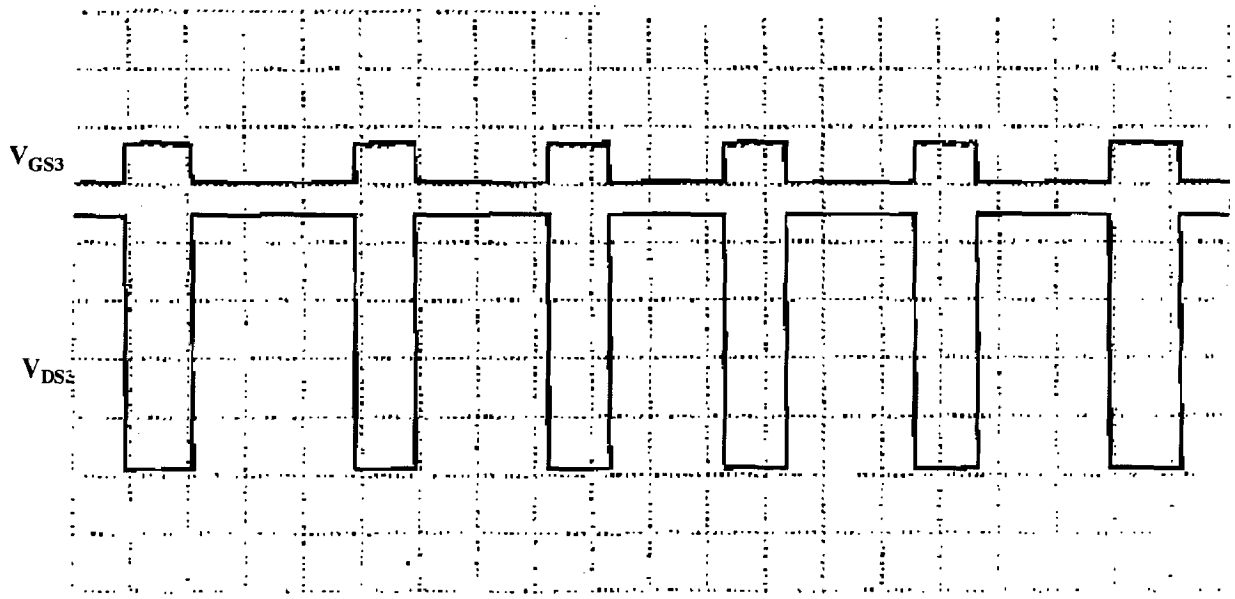

Fig 5.23(c)

Fig 5.23 Waveforms for the V_{DS} and V_{GS} for three Mosfets when the pulses from the 8255 are fed

The switched reluctance motor has attractive potential for variable speed applications, in view of its robustness, simple construction and fault tolerance. Different simulation models are presented along with the simulation with and without using the MATLAB/Simulink block of SRM. The simulation of SRM drive for load variations and reference speed variations was carried out. Fuzzy logic controller was also used to determine the speed response.

Investigations were carried out to determine the significance of the switching angles. Optimum switching angles were determined with rigorous emphasis on the performance indices. The maximum turn off angle that can be used for a rated load torque is determined. Also, the maximum load that can be applied for this angle is determined. The affect of turn on angle on the speed response is investigated.

Implementation of Microcontroller controlled SRM drive is done experimentally. The control signals from the microcontroller are generated based on the rotor position. Power converter is fabricated and is interfaced to the microcontroller through the signal conditioning circuit to the speed encoder. The 8031 microcontroller was used for the work. The timer is programmed in order to get the control signals based on the pulses obtained to it from encoder. The output signals are obtained at the pins of 8255. The start up algorithm and control algorithm for motor operation are explained through flowcharts.

6.1 Future Scope [41-44]

In this thesis, microcontroller is used for the controlling purpose. A DSP based implementation can be done which gives many control features to the drive. The speed encoder can be directly interfaced to the DSP kit. It reduces lot of hardware such as there is an inbuilt ADC in it, also many controllers can be easily implemented in it. An SRM drive with bidirectional rotation can extended as a future. A sensorless SRM can also be modeled if the magnetization characteristics are available.

[1] Krishnan, R., "*Switched Reluctance Motor Drives: Modeling, Simulation, Analysis, Design, and Applications*", CRC Press, 2001.

[2] Timothy L. Skvarenina, "*The Power Electronics Handbook*", CRC Press, 2002.

[3] Bhimbra.P.S., "*Generalized Theory of Electrical Machines*", Khanna Publishers, 2002.

[4] Jun-Young Lim, Yun-Chul Jung, Sang-Young Kim and Jung-Chul Kim, *"Single Phase Switched Reluctance Motor for Vacuum Cleaner"*, ISIE 2001, Pusan, KOREA, pp.1393-1400.

[5] Jifeng Han, Xiaolin Zhou, Annette von Jouanne, Alan Wallace, *"Design of an SRM-Based Actuator for High-Performance Steering Vane Control on the Landing Craft Air Cushion (LCAC) Hovercraft "*, IAS, 0-7803-8486-5/04/$20.00 © 2004 IEEE, pp. 1598-1601.

[6] Kim Jong-Han Lee, Jun-Ho Eun-Woong Lee, *"Design of the Single Phase SRMfor the Blower Considering Self-starting"*, Department of Electrical Engineering, Chungnam National University, Daejeon, Korea .

[7] Nobuyuki Matsui, Takashi Kosaka, Norimoto Minoshima and Yasuharu Ohdachi, *"Development of SRM for Spindle Motor System"*, 0-7803-4943-1/98/$10.00 0 1998 IEEE, pp. 580-585.

[8] Jun-Young Lim, Yun-Chul Jung, Sang- Young Kim,Yong- Won Choi, Jung-Chul Kim, *"High Efficiency and Low-Cost Switched Reluctance Motor for Air-conditioner Blower"*, 0-7803-7156-9/02/$10.000 2002 IEEE , pp. 1460-1467.

[9] J. Wolff, R. Rahner, H. Späth, *"Sensorless Speed Control of A Switched Reluctance Motor for Industrial Applications"*, Optimization of Electrical and Electronic Equipments - Brasov 1998, Volume 2, pp. 457-462.

[10] Slobodan Vukosavic and Victor R. Stefanovic, "SRM Inverter Topologies: A Comparative Evaluation ," IEEE Trans. Ind. Appl., vol. 27, no.6 Nov/ Dec 1991, pp.1034-1047.

[11] Arthur V. Radun, *"Design Considerations for the Switched Reluctance Motor"*, IEEE Transactions on Industry Applications, vol. 31, no. 5, September/ October,1995, pp. 1079-1087.

[12] B. Fahimi, *"Design of Adjustable Speed Switched Reluctance Motor Drives"*, IECON'01: The 27th Annual Conference of the IEEE Industrial Electronics Society, pp. 1577- 1582.

[13] M. N. Anwar, Iqbal Husain, Arthur V. Radun, *"A Comprehensive Design Methodology for Switched Reluctance Machines"*, 0-7803-6401-5/00/$10.00 0 2000 IEEE, pp. 63-70.

[14] F. Soares, P. J. Costa Branco, *"Simulation of a 6/4 Switched Reluctance Motor Based on Matlab/Simulink Environment"*, IEEE Transactions on Aerospace and Electronic Systems, VOL. 37, No. 3, JULY 2001, pp. 989-1009.

[15] Hamid Ehsan Akhter, Virendra K. Sharma, A. Chandra, and Kamal Al-Haddad, *"Performance Simulation of Switched Reluctance Motor Drive System Operating With Fixed Angle Control Scheme"*, Electrimacs 2002, August 18-21, Switched Reluctance Motors.

[16] Liuchen Chang, *"Modelling of Switched Reluctance Motors"*, CCECE'97, 0-7803-3716-6/97/$5.00 0 1997 IEEE, pp.866-869.

[17] J. Mahdavi, G. Suresh, B. Fahimi, M. Ehsani, *"Dynamic Modeling of Non-Linear SRM Drive with PSPICE"*, IEEE Industry Applications Society Annual Meeting 5-9, 1997 New Orleans, Louisiana, October 5-9, 1997, pp. 661-667.

[18] O. Ichinokura, T. Onda, M. Kunura, T. Watanabe, T. Yanada and H.J. Guo, *"Analysis of Dynamic Characteristics of Switched Reluctance Motor Based on SPICE"*, IEEE Transactions on Magnetics, VOL 34, NO 4, JULY 1998, pp.2147-2149.

[19] H. Chen, J. Jiang, D.Zhang and S. Sun, *"Models and Simulation of the Switched Reluctance Motor Drive with the Microcomputer Control Based on MATLAB Software Package"*, 0-7803-6253-5/00/$10.00 02000 IEEE, pp. 493-496.

[20] Tauter T. Borges, Darizon A. de Andrade, Harold R. de Azevedo & Lucian0 M., *"Switched Reluctance Motor drive at high speeds, with control of current"*, 0-7803-39464/97/$10.00 0 1997 IEEE, pp. TB1 12.1- TB1 12.3.

[21] Chong- Chul Kim, Jin Hur, Dong- Seok Hyun, *"Simulation of a Switche Reluctance Motors Using Matlab/ M-file"*, 0-7803-7474-6/02/$17.00 @ 2002 IEEE, pp.1066- 1071.

[22] Phop Chancharoensook, Muhammed F Rahman, *"Dynamic modeling of a Four-Phase 8/6 Switched Reluctance Motor using Current and Torque Look-Up Tables"*, 0-7803-7474-6/02/$ 17.00 @ 2002 IEEE, pp. 491- 496.

[23] Hamid Ehsan Akhter, Virendra K. Sharma, Ambrish Chandra, Kamal Al-Haddad, *"Modeling Simulation and Performance Analysis of Switched Reluctance Motor Operating with Optimum Value of Fixed Turn-On and Turn-off Switching Angles"*, 0-7803-7754-0/03/$17.00 @2003 IEEE, pp. 397- 402.

[24] Syed A. Hossain, Iqbal Husain, *"Modeling, Simulation and Control of Switched Reluctance Motor Drives"*, 0-7803-7906-3/03/$17.00 02003 IEEE, pp. 2447- 2452.

[25] I. El-Samahy, M. I. Marei and E. F. El-Saadany, *"Dynamic Simulation of a Switched Reluctance Motor Drive on EMTDC/PSCAD Software"*, 0-7809-9156-X/05/$20.00 @ 2005 IEEE, pp. 1-8.

[26] Mohamed N. AbdulKadir, AbdulHalim Mohd. Yatim, *"Maximum Efficiency Operation Of Switched Reluctance Motor By Controlling Switching Angles"*, 7803-3773-5/97/$10.00 @ 1997 IEEE.

[27] Suying Zhou, Hui Lin, *"Modeling and Simulation of Switched Reluctance Motor Double Closed Loop Control System"*, Proceedings of the 6th World Congress on Intelligent Control and Automation, June 21 - 23, 2006, Dalian, China, pp. 6151-6155.

[28] Silverio Bolognani and Mauro ZigliottoFuzzy, *"Fuzzy Logic Control of a Switched Reluctance Motor Drive"*, IEEE Transactions on Industry Applications, VOL. 32, NO. 5, September/October 1996, pp. 1063-1068.

[29] Adnan Derdiyok, Nihat Inang, Veysel Ozbulur, Halit Pastacl, M. Orug Bilgig, *"Fuzzy Logic Based Control of Switched Reluctance Motor to Reduce Torque Ripple"*, 0-7803-3946-0/97/S10.00 O 1997 IEEE, pp. TB1 9.1 – TB1 9.3.

[30] Sung-Jae Huh, Kyu-Dong Kim, Huh Uk-You1 Huh, Joon-Hyun Jang, Byung-Suk.Lee, Woo-Yong.Chung, *"Fuzzy Logic Based Control of High Current SRM"*, SICE 2002 Aug. 5-1.2WZ Osaka, pp. 1216-1219.

[31] Li ZHENG, *"A Practical Guide to Tune of Proportional and Integral(P1) like Fuzzy Controllers"*, 0-7803-0236-2 I92 $3.00 Q 1992 IEEE, pp. 633-640.

[32] Nihat Inang, Adnan Derdiyok, Veysel Ozbulur, Nurettin Abut, Fahrettin Arslan, "Torque Ripple Reduction of a Switched Reluctance Motor Including Mutual Inductances", IEEE Catalog Number: 97TH8280, ISIE'97 - Guimariies, Portugal, 489-492.

[33] K. J. Tseng and Shuyu Cao, "A SRM Variable Speed Drive with Torque Ripple Minimization Control", 0-7803-6618-2/01/$10.00 0 2001 IEEE, pp. 1083-1089.

[34] Virendra Kumar Shanna, Bhim Singh, S.S. Murthy, *"Development of A Simple Analog Controller For Switched Reluctance Motor"*, 0-7803-5812-0/00/$10.00Q 2000 IEEE, pp. 595-599.

[35] B.K.Bose, T.J.E. Miller, P.M. Szczesny and W.H. Bicknell, "Microcomputer control of Switched Reluctance Motor", IEEE/IAS Annual Meeting, 1985, pp. 542-547.

[36] Sung-Jun Park, Jac-Won Moon, Han-Woong Park and Jin- Woo Ahn, " *Microcontroller based Single-phase SRM Drive with High Power Factor"*, 0-7803-7369-3/02/$17.00 (c) 2002 IEEE, pp.701-705.

[37] Feel-Soon Kang, Sung-Jun Park, Han-Woong Park, Soon-Ill Hong, and Cheul-U Kim, *"Linear Grade Encoder for High Resolution Angle Control of SRM Drive"*, IEEE Catalogue No. 01 CH37239, 0 2001 IEEE, 549-555.

[38] Hamid Ehsan Akhter, Virendra K. Sharma , A. Chandra, and Kamal Al-Haddad, *"Performance Simulation of Switched Reluctance Motor Drive System Operating With Fixed Angle Control Scheme"*, Electrimacs 2002, August 18-21, Switched Reluctance Motors.

[39] Shun-Chung Wang, Wen-Han Lan, *"A PC-Based Apparatus for Identifying Magnetization Characteristics of Switched Reluctance Machines"*, VECIMS 2004- IEEE International Conference on Virtual Environments, Human-Computer Interfaces, and Measurement Systems Boston, MA, USA, 12-14 July 2004, pp. 107-112.

[40] S K Mondal, S N Saxena , S N Bhadra and B P Muni, *"Evaluation Of A Novel Analog Based Closed-Loop Sensorless Controller For Switched Reluctance Motor Drive"*, 0-7803-7116-X/01/$10.00 (c) 2001 IEEE, pp. 2073-2080.

[41] 56F8300 3-Phase Switched Reluctance Motor Control with MC56F8300 16-bit Digital Signal Controllers, freescale.com.

[42] Digital Signal Processing Solutions for the Switched Reluctance Motor, bpra058, Texas instruments.

[43] Implementation of a Current Controlled Switched Reluctance Motor Drive Using TMS320F240, APPLICATION REPORT: SPRA282, Texas Instruments.

[44] Switched Reluctance Motor Control – Basic Operation and Example Using the TMS320F240, Application Report SPRA420A - February 2000, Texas Instruments.

[45] 8031/V51 Anshuman User's Guide.

Appendix I

Motor details:

Stator poles, NS=6;

Rotor poles, NR=4;

No: of phases, P=3;

DC link voltage, V=150;

Phase resistance, R=1.30;

Rotor Inertia, J=0.0013 Kg/m2;

Friction constant, F=0.0183 N-m/ rad/ sec;

Minimum inductance, L_{MIN}=8 m H;

Maximum inductance, L_{MAX}=60 m H;

Appendix II:

Motor details:

Stator poles, NS=6;

Rotor poles, NR=4;

No: of phases, P=3;

DC link voltage, V=240;

Phase resistance, R=0.01;

Rotor Inertia, J= 0.0082 Kg/m2;

Friction constant, F=0.01 N-m/ rad/ sec;

Minimum inductance, L_{MIN}=0.67 m H;

Maximum inductance, L_{MAX}=23.6 m H;

Maximum current =450 A

Maximum flux linkages= 0.486 V-sec

Appendix III:

Microcontroller [45]:

The micro-processor such as Intel's x86 family or Motorola's 680x0 family contain no RAM, no ROM, no I/O ports on the chip itself. For this reason, they are commonly referred to as general-purpose microprocessors. On the other hand the Micro controller has CPU (a microprocessor) in addition, a fixed amount of RAM, ROM, I/O ports, and timers embedded together on one chip. The fixed amount of on-chip ROM, RAM, and number of I/O ports in micro controllers makes them ideal for many applications in which cost and space are critical.

In many applications, for example a TV remote control, there is no need for the computing power.

In addition, in many applications, the space it takes, the power it consumes, and the price per unit are much more critical considerations than the computing power. These applications most often require some I/O operations to read signals and turn on and off certain bits. Therefore, for all these reasons the microcontrollers are best option where cost and space are critical.

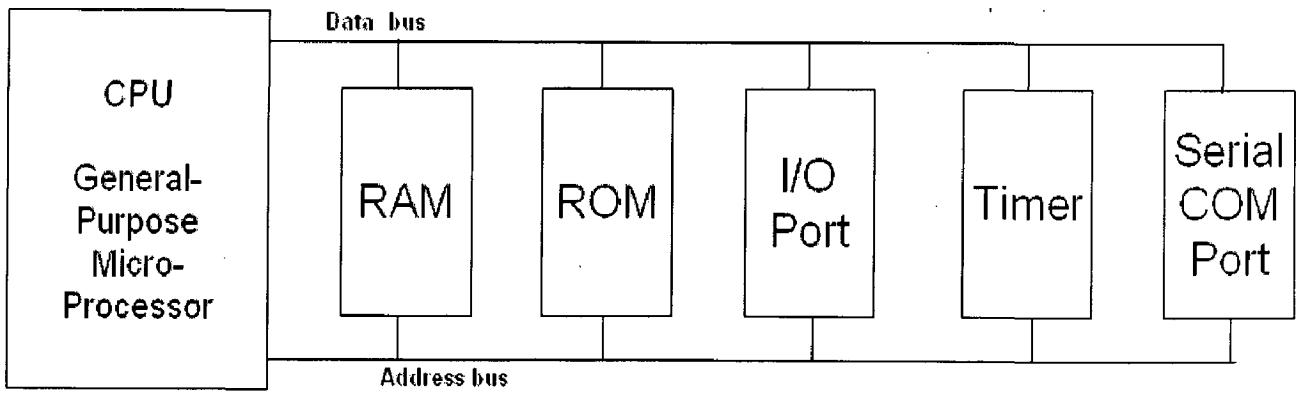

Fig: 4.1 General-Purpose Microprocessor Systems

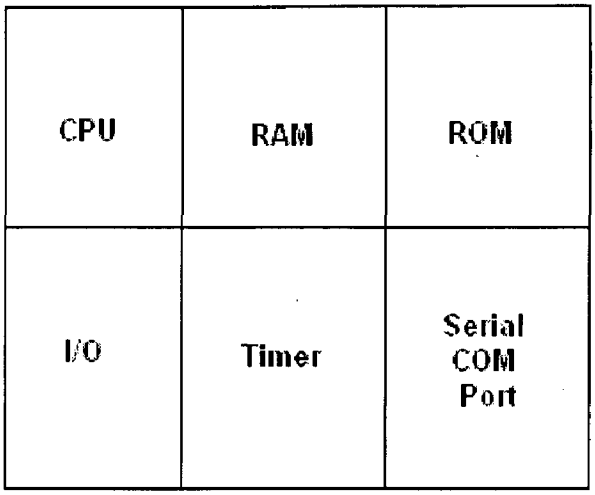

Fig: 4.2 Microcontrollers

Microcontroller 8031 has been used for the implementation of the project. It is an 8 bit microcontroller. In 1981, Intel Corporation introduced an 8-bit microcontroller called 8051 which is the original member of the 8051 family. The other two members of the 8051 family are 8052 and 8031.

A comparison of 8051 family members is given below:

Feature	8051	8052	8031
ROM (on-chip program space in bytes)	4K	8K	0K
RAM (bytes)	128	256	128
Timers	2	3	2
I/O Pins	32	32	32
Serial Ports	1	1	1
Interrupt sources	6	8	6

8031 chip is referred to as ROM-less 8051.

A brief contrast between 8031 and 8085 is given below:

8031 Vs 8085:

1. 8031 has got four register banks (R0-R7), unlike 8085.

2.8031 have only one 16-bit pointer, "DPTR" unlike 8085, which has three pointer namely (BC, DE, HL).

3. Both 8031 & 8085 have registers A and B, but instead of C, D, E, H, L in 8085, 8031 has registers (R0-R7).

4. 8031 has internal RAM of 120Kbytes unlike 8085.

5. 8031 doesn't provide direct addressing mode while 8085 does.

6. Internal RAM in 8031 can be addressed in Register indirect mode.

7. 8031 has four built in, 8 bit I/O ports.

8. 8031 (8032) has two (three) built in, 16 bit Timers/ Counters.

9. 8031has instruction to access "Bits" in Internal RAM & SFRs.

The above comparison shows that the 8031 microcontroller is much more versatile as compared to 8085.